Jour. Fac. Sci., Hokkaido Univ., Ser. IV,
vol. 16, no. 4, Feb., 1975, pp. 367-420.

THE BASIC PLUTONIC ROCKS OF THE HIDAKA METAMORPHIC BELT, HOKKAIDO. PART I

by

Seiji Hashimoto

(With 3 plates and 46 text-figures)

(Contribution from the Department of the Geology and Mineralogy
Faculty of Science, Hokkaido University, Sapporo: No. 1380)

CONTENTS

Introduction and General Geologic Setting

The axial belt of Hokkaido is characterized by the occurrence of two metamorphic belts which strike parallel with each other in a N-S direction. The metamorphic belt in the west is called the Kamuikotan Belt and is characterized by the association of glaucophane schist and lawsonite bearing greenschist accompanied by metagabbro and serpentinite. The eastern belt, the Hidaka Metamorphic Belt, consists of migmatitic rocks and plutonic rocks ranging in composition from peridotitic, gabbroic to granitic. These two

metamorphic belts crop out within a thick pile of probable Triassic to Jurassic geosynclinal deposits, called the Hidaka Supergroupd which is considered to form two anticlinal crests along which the two metamorphic belts are exposed. The "crests" are separated from one another by a narrow but continuous synclinal trough which is filled with Cretaceous sediments corresponding to Albian and Maastrichian age.

The Hidaka Supergroup has been divided into three successive stratigraphic units as follows: The Nakanokawa Group (Lower), the Kamui Group (Middle) and the Sorachi Group (Upper).

The Nakanokawa Group occurs exclusively along the eastern side of the Hidaka Metamorphic Belt which separates the deposits with those in the west and is composed of flysch-like deposits of sandstone and slate alternations. The sediments are folded to form open folds, the axes of which run in a NNW direction in the southern part and trend to the NE in the northern part of the eastern flank. Overturned folds and traverse faulting are seen where the strike direction turns toward the east. The rocks have been thermally metamorphosed from 2 to 4 km close to the metamorphic belt and parts seem to have been transformed into migmatite. However, the sediments are obliquely cut by the eastern most margin of the metamorphic belt which is delineated by a distinct fault or sheared zone.

The geosynclinal deposits along the western flank of the Hidaka Metamorphic Belt have been called the Kamui Group which comprises black slate, sandstone and associated limestone. The Kamui Group is overlain by a thick deposit of the Sorachi Group consisting of schalstein, pillow lava, diabase, chert and limestone. The sediments have been intensely folded and sheared towards the west so that many eastward dipping thrusts, both large and small, are present.

The Kamui and Sorachi Group deposits are considered to be eugeosynclinal and contrast with those of the Nakanokawa Group which are probably miogeosynclinal.

Therefore, the Hidaka Metamorphic Belt crops out along the junction of two distinct depositional basins in a geosynclinal trough forming a thick plank-like belt of plutonic rocks that have been upthrust towards the west (Fig. 44).

Previous work

The Hidaka Metamorphic Belt had attracted the attention of geoligists since 1891, when Jimbo (1891) regarded the belt as forming the Archean basement of Hokkaido. Oinoue (1918) summarized the earlier work and postulated

that the present metamorphic belt comprised an intrusive zone of granite which was injected into palaeozoic sediments. Suzuki (1944) postulated a similar version but stressed the difference in metamorphism between the Hidaka Belt and the Kamuikotan Belt to the west. In the 1940's, the first detailed surveys were carried out in the Hidaka Metamorphic Belt. During this time the widespread occurrence of the migmatite and basic rocks were mapped in many areas that had previously been considered to be granitic batholith (Hunahashi 1951, Hashimoto 1949). The close tectonic relationship between the Hidaka and Kamuikotan metamorphic belts was realized at this time, (Hunahashi and Hashimoto 1951).

This work was further elaborated by Hunahashi when he established the framework of "Alpine Orogenesis" in Hokkaido (Hunahashi, 1957). Hunahashi stressed the significance of migmatite in the Hidaka belt from the geosynclinal to the orogenic stage and discussed the development of the geology of Central Hokkaido with reference to the Hidaka Orogeny.

Sako (1963), postulated that two stems of basic rocks exist in the Hidaka Metamorphic Belt; the olivine gabbro stem and the dioritic gabbro stem. According to him the olivine gabbro stem includes not only gneissose gabbros but also metagabbro and peridotite, the intrusion of which was correlated with the stage of gneiss formation.

Rocks of the dioritic gabbro stem were intruded at a later stage, synchronus with the formation of migmatite. Sako also considered that the relationship between diabase sheets in the geosynclinal sediments and the amphibolite of the Hidaka Metamorphic Belt might be the same rocks but differing in the level of exposure.

In this paper, the characteristics of field occurrence of the various basic rocks in the Hidaka Metamorphic Belt through time and space will be considered. The petrology of the rocks will be given in a forthcoming paper.

Division of the Hidaka Metamorphic Belt

The Hidaka Metamorphic Belt can be divided into three zones on the basis of tectonics and rock type. These zones are, from west to east; (1) The Western Zone, (2) The Axial Zone and (3) The Eastern Zone (Tab. 1).

(1) The Western Zone

This zone is 5km to 0.5km wide and some 120km long. It runs parallel to the strike of folded geosynclinal sediments of Kamui Group to the west and is bordered by gneisses of the Axial Zone to the east. The western margin is

Table 1

	BASIC ROCKS		GNEISSES, MIGMATITES AND GRANITIC ROCKS
	The Western Boundary Thrust		
The Western Zone	Greenschist		
	Biotite Amphibolite		
	Green Hornblende Schistose Amphibolite		
	Metagabbro, Layered Gabbro and Gabbroic Amphibolite		
	Green Hornblende Amphibolite		
	Ultrabasic Rock		
The Axial Zone	Type I Septa		
	Brown Hornblende Amphibolite Schistose Gabbro	Banded Biotite Amphibolite Biotite bg. Amphibolite Biotite Hornblende Gneiss Pyroxene Amphibolite	Porphyroblastic Plagioclase-Biotite Gneiss
	Type I Gneissose Gabbro	Gneissose Olivine Gabbro Gneissose Gabbro Gneissose Norite	
	Type II Septa		
	Type II Gneissose Gabbro	Olivine Gabbro Gabbro Norite	Migmatite and Banded Biotite Gneiss
The Eastern Zone	Type III Septa		
	Normal Gabbro	Olivine Gabbro Gabbro Norite Hornblende Gabbro Diorite	Gneissose Granite
	Layered Gabbro (AME-YAMA)		Granite

defined by a thrust and narrow continuous outcrops of sedimentary greenschist. The eastern margin is marked by the presence of elongated, discontinuous ultramafic lenses.

The Western Zone is divided into five subzones characterized by the following rocks from west to east. Each subzone is bounded by thrust faults.

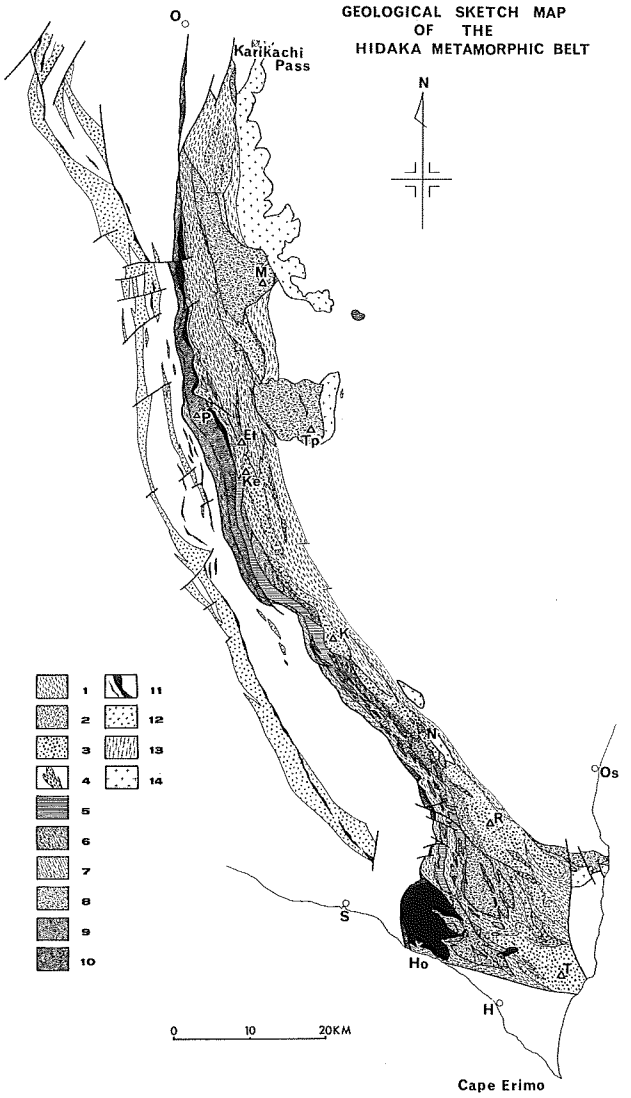

Fig. 1 Geologic Sketch Map of the Hidaka Metamorphic Belt

1. Gneiss 2. Migmatitic Gneiss 3. Migmatite 4. Migmatite (intrusive type) 5. Brown Hornblende Amphibolite 6. Biotite Hornblende Gneiss 7. Gneissose Gabbro 8. Normal Gabbro 9. Amphibolite of the Western Zone 10. Metagabbro including Layered Gabbro 11. Ultrabasic rock 12. Diabase 13. Gneissose Granite 12. Granite

M: Mt. Memuro P: Mt. Poroshiri Et: Mt. Esaoman-Tattabetsu Tp: Mt. Tokachi-Poroshiri Ke: Mt. Kamuiekuchikaushi K: Mt. Kamui N: Mt. Notsuka R: Mt. Rakko T: Mt. Toyoni

O: Ochiai Os: Oshirabetsu S: Samani Ho: Horoman H: Horoizumi

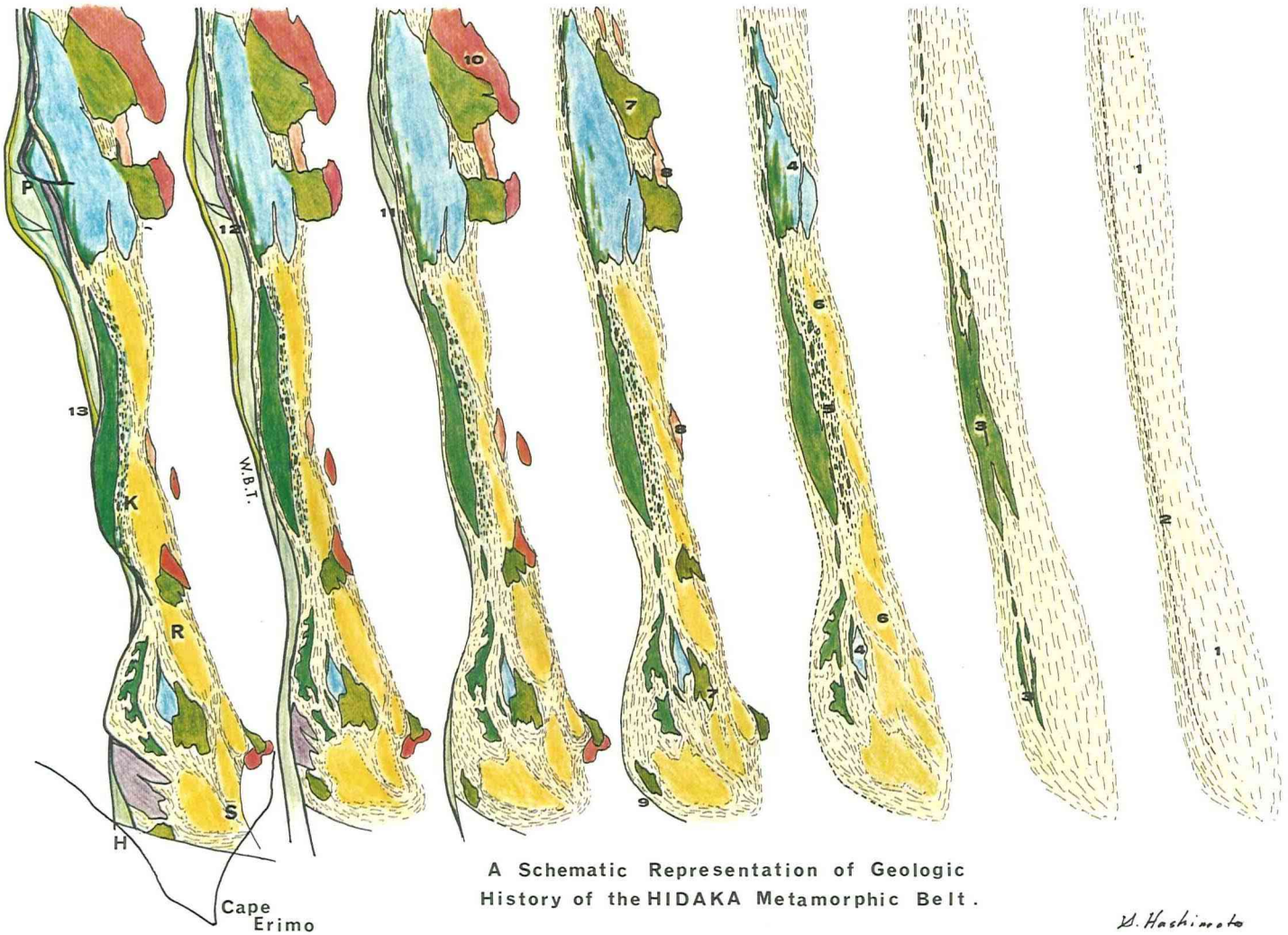

A Schematic Representation of Geologic History of the HIDAKA Metamorphic Belt.

D. Hashimoto

1973

Pl. I A Schematic Representation of the Geologic History of the Hidaka Metamorphic Belt.

(Width and length of rock units is arbiterally fixed on the basis of the present outcrops.)

1. Beginning of the metamorphism is indicated by formation of plagioclase porphyroblastic biotite gneiss.
2. Shearing movement occured particularly along the western margin of the gneiss belt.
3. Intrusion of diabase sheets which were successively metamorphosed to form brown hornblende amphibolite.
4. At both ends of the metamorphic belt, the intrusion of brown hornblende amphibolite was followed by concordant injection of gneissose olivine gabbro and norite.
5. Migmatitic activity was active within the gneiss belt and resulted in the converting of the brown hornblende amphibolite to the east to biotite-hornblende gneiss.
6. At this stage embryonic migmatite domes or bilges were formed.
7. Discordant successive intrusion of olivine gabbro, pyroxene and hornblende gabbro. Diorite was formed by mixing of basic and acidic magma, the latter of which may have originated by remobilization of migmatite.
8. Intrusion of gneissose granite derived from a migmatitic source.
9. Beginning of thrusting movement in Horoman area.
10. Intrusion of post-kinematic granite.
11. Intense thrusting along the western margin of the metamorphic belt might have begin at this stage. The thrusting was accompanied by the tectonic intrusion of layered gabbro from deeper levels.
12. The gabbroic rocks were metamorphosed to form green hornblende amphibolites during differential uplift and deformation.
    Preliminary stage of the formation of Western Boundary Thrust.
13. In places, subsequent thrusting resulted in plagioclase porphyroblastic biotite gneiss and brown hornblende amphibolite overthrusting the Western Boundary Thrust.

Locality P: Mt. Poroshiri K: Mt. Kamui R: Mt. Rakko
S: River Saru Area H: Horoman Area

Subzone	A	Epidote amphibolite
"	B	Green hornblende schistose amphibolite
"	C	Gabbroic amphibolite and meta-gabbro
"	D	Green hornblende amphibolite
"	E	Ultramafic rocks

A. Epidote Amphibolite

The epidote amphibolite is about 100m in width and is particularly well exposed in the northern and central parts of the metamorphic belt. The disappearance of these rocks together with the greenschist and other members of the amphibolite group in some areas is due to westward overthrusting at a later time. The epidote amphibolite is typically, fine-grained and compact and composed of bluish-green acicular hornblende, granular epidote, sphene, Fe-ore and plagioclase (An_{25-20}). Actinolite occurs as large grains, and is replaced in various degrees by bluish-green hornblende (Fig. 5), (R Grapes. et. al. submitted for publication).

The contact between epidote amphibolite and green hornblende schistose amphibolite to the east, is gradational in the north-western part of the Poroshiri-dake plutonic complex, but is typically faulted elsewhere. This change may be marked by an abrupt change in the direction of foliation (Watanabe, J., 1961).

B. Green Hornblende Schistose Amphibolite

Green hornblende schistose amphibolite varies from 500m to 1km width. The typical rock of this amphibolite is rather fine-grained and compact with many leucocratic plagioclase veins parallel to the schistocity. Aligned pods or lenses composed of coarse-grained hornblende and plagioclase are common. Many of these coarse-grained pods and lenses end abruptly, while some are continued into veins which are rimmed by hornblende. The coarse-grained bodies show deformation, and they may have formed by remobilization of the amphibolite during metamorphism.

The green hornblende schistose amphibolite mainly consists of green, dark green or bluish-green hornblende and granular plagioclase, accompanied by aggregates of granular sphene and Fe-ore (Fig. 6). Epidote is not a normal constituent but is sometimes present in veins or pods with rare diopside.

The green hornblende schistose amphibolite is transitional into gabbroic amphibolite. Alternation of both rock types occur very commonly. Existence of relicts of gabbroic amphibolite in the green hornblende schistose amphibolite indicates that the latter was formed from the gabbroic amphibolite by dynamic metamorphism during uplift.

C. Metagabbro and Gabbroic Amphibolite

To the east of the green hornblende schistose amphibolite a broad composite belt consisting of metagabbro and gabbroic amphibolite, some 2 to 3km wide and 60km long, exists. In many localities eastward dipping thrusts are present. Narrow bands of biotite schist, porphyroblastic plagioclase-biotite gneiss and in one locality, manganiferrous schist, are found near the western margin of zone.

In places weakly metamorphosed olivine gabbro and troctolite, often showing layering, are exposed (Fig. 3,4). The layered gabbroic mass centred on Mt. Poroshiri, is the largest and most typical outcrop of this kind and well developed rhythmic layering between wehrite, troctolite and anorthosite is exposed over some 1500km (Miyashita, S., in this volume). The Mt. Poroshiri layered gabbro is fault bounded and probably represents a large tectonic block which was uplifted to the present level with minimum deformation. In many other localities well preserved layered structures are preserved but the rock is totally converted to amphibolite.

The typical gabbroic amphibolite consists of partly recrystallized blastoporphyritic plagioclase (An_{70}), pyroxene, actinolitic amphibolite with minor epidote, sphene and shows a complete gradation into meta-gabbro (Fig. 7).

Fig. 2 Gabbroic amphibolite showing a pegmatitic segregation replacing amphibolite.

During amphibolitization, the metagabbro and gabbroic amphibolite are replaced by irregular seams or lenses of pegmatoid with subidiomorphic plagioclase and subophitic hornblende. Some of pegmatoid amphibolites are comformably foliated with host rocks suggesting that they have been formed by remobilization of the host metagabbro and gabbroic amphibolite (Fig. 2).

Amphibolites associated with the layered gabbro of the Mt. Poroshiri area are, for the most part, massive, heterogeneous in mineral composition, and preserve original textural features of the gabbro. The mineralogical changes involved are very complex and are controlled by the original composition. Spinel, corundum, rhombic pyroxene, anthophyllite, hornblende, chlorite and penninite are the products formed by reaction of the plagioclase and mafic minerals and will be described in separate paper.

D. Green Hornblende Amphibolite

Green hornblende amphibolite crops out as a discontinuous belt extending some 15km in the Mt. Poroshiri area. It is in fault contact with the metagabbro-gabbroic amphibolite to the west and is bounded by peridotite-dunite to the east. The foliation of the green hornblende amphibolite strikes in a N-W to S-E direction and parallels to the strike and dip of the ultrabasic rocks.

The typical green hornblende amphibolite is homogeneous in texture, and also in mineral composition, being free from leucocratic bands or pegmatoid segregations. The rock consists of nematoblastic deep green hornblende and the plagioclase (about An_{50}) accompanied by accessory amount of sphene and Fe-ores (Fig. 8) Diopside is sometimes present and is associated with green hornblende with? cummingtonite exsolution lamellae and ends.

E. Ultramafic Rocks

The eastern boundary of the Western Zone is marked by thrust, the existence of which is emphasized by elongated ultramafic bodies. The ultramafic bodies are typically concentrated in areas adjacent to the gneissose gabbroic complexes, and appear to be proportional to the surface outcrops of the gneissose gabbro and to the distribution of metagabbros and amphibolites.

With the exception of the Horoman Complex, almost all of the ultramafic bodies appear to be sheet-like in form. No contact metamorphism is present in the rocks adjacent to the ultramafics. Most of the ultramafic bodies are foliated or granulated indicating that their mode of emplacement was tectonic.

In Wensaru River area, Northern Hidaka's, the ultramafics layered from dunite-perioditite-plagioclase peridotite (Nochi and Komatsu, 1967) and are similar to the well-developed layering in the Horoman body in the southern

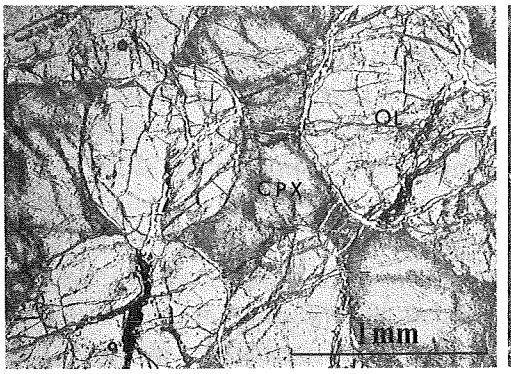

Fig. 3 Photomicrograph of wehrlite part of the layered gabbro, Mount Poroshiri.
All microphotographs are represented in the same scale as is exhibited in this figure.

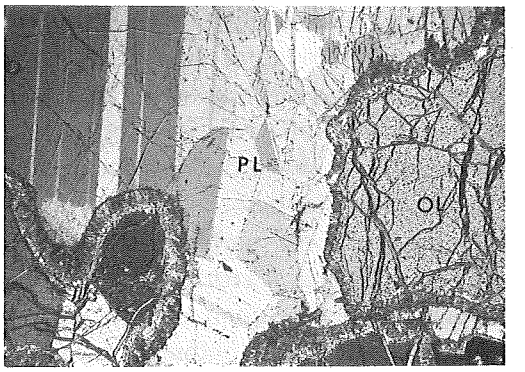

Fig. 4 Troctolitic part of the layered gabbro, Mount Poroshiri.
Note the reaction line between plagioclase and olivine.

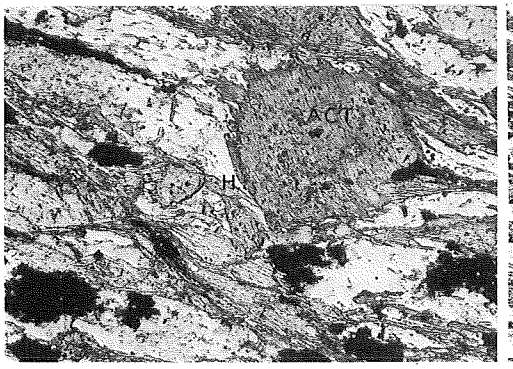

Fig. 5 Epidote amphibolite.
Actinolite is surrounded by elongated bluish-green hornblende(H).

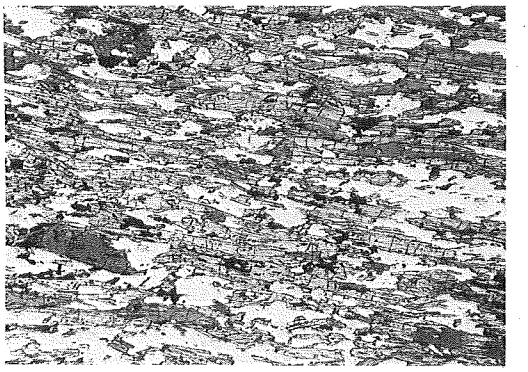

Fig. 6 Green hornblende schistose amphibolite.

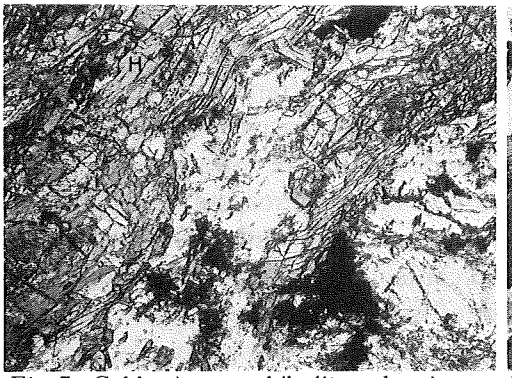

Fig. 7 Gabbroic amphibolite showing blastoporphyritic plagioclase, and pale greenish hornblende(H) containg relict of clinopyroxen(P).

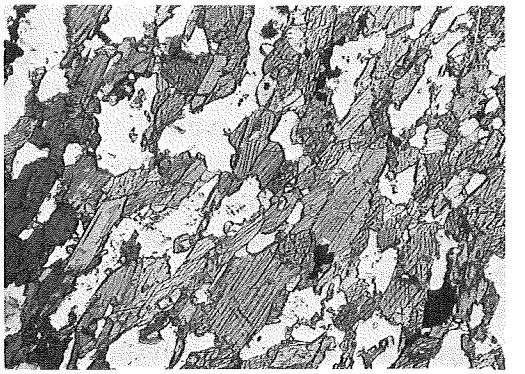

Fig. 8 Green hornblende amphibolite (Eastern margin of the Western Zone) showing completely recrystallized texture.

extremity of the Hidaka Metamorphic Belt (Komatsu and Nochi 1967, Niida, 1974).

The ultramafic rocks of the Hidaka Metamorphic Belt include dunite, lherzolite and harzburgite. Olivine (around Fo_{90}) is present in all of the rock types. Those varieties rich in plagioclase contain clinopyroxene rather than orthopyroxene. Diopsidic pyroxene from Wensaru peridotite may be of mantle origin (Komatsu, submitted for publication). For further mineralogical data the reader is refered to Komatsu and Nochi. The detailed genesis of the ultramafic are not known at present.

(2) The Axial Zone

Basic rocks of the Axial Zone are represented by the following rock types
A. Brown hornblense amphibolites and schistose gabbro
B. Gneissose gabbro

A. Brown hornblende Amphibolite

Rocks belonging to this group are characterized by the occurrence of brown hornblende with the exception of amphibolite which crops out in the southern part of the metamorphic belt. The brown hornblende amphibolites occur as sills or sheets associated with porphyroblastic plagioclase-biotite gneiss and/or migmatite. They are metamorphosed in various degrees or have been affected by metasomatism.

Several varieties can be distinguished on the basis of mineral composition and geological relations.

In the southern part of the metamorphic belt, especially around the Mt. Rakko and Horoman areas, the following types of amphibolite are present.

(a) Banded biotite amphibolite.
(b) Type I Brown hornblende amphibolite, (Senso strico.).
(c) Type II Brown hornblende amphibolite and associated cordierite-hypersthene-biotite amphibolite.
(d) Anthophylite amphibolite.
(e) Biotite-hornblende gneiss.

Near the Mt. Poroshiri plutonic complex in the northern part of the metamorphic belt, schistose gabbro, pyroxene amphibolite are associated with brown hornblende amphibolite and biotite-hornblende gneiss.

(a) Banded biotite amphibolite

Sheets or lenses of this amphibolite exclusively occur along the western margin of the zone of porphyroblastic plagioclase-biotite gneiss near the Western Boundary Thrust. The rocks have a marked schistosity and are

characterized by thin bands of gneiss which alternate with amphibolite. The banded biotite amphibolite is nematoblastic to schistose in texture and is completely recrystallized so that no relict minerals or textures remain. The rock consists of green to olive green hornblende, granular grains of turbid plagioclase and epidote. The hornblende is typically replaced by fine dark greenish biotite. Quartz may be present (Fig. 10).

(b) Type I Brown hornblende amphibolite

This rock crops out as conformable sheets to the east of the banded biotite amphibolite and forms a distinct zone. The largest sheet (up to 1.5km in width) extends from the western slope of Mt.Kamuiekuchikaushi to Mt. Kamui, over a distance of some 40km, in the middle part of the metamorphic belt (Fig. 1). From both the southern and northern extremities of this sheet, swarms of thin sheets, typically 10m–50m wide extend parallel to the strike of the surrounding gneiss. The sheets are generally steeply dipping, but those in the southern area generally dip gently to the east and are metamorphosed in various degrees. Biotite and quartz are common in the marginal parts of the sheets.

Least altered brown hornblende amphibolites are massive, homogenerous rocks, consisting of coarse-grained xenomorphic hornblende and granular plagioclase which are commonly zoned from An_{60-50} to An_{48}. The hornblende also typically has a zonal structure with brown to greenish brown cores and pale green-brown margins which contain exsolution lamellae of ? cummingtonite (Fig. 11). Some amphibolites have a relict medium-grained ophitic texture although recrystallization has caused the plagioclase to become xenomorphic in part.

The eastern part of the largest sheet described above, has suffered migmatization to form a heterogeneous biotite hornblende gneiss which contains abundant streaks or lenses of the original amphibolite. Agmatitic amphibolites characterized by an aggregate of angular fragments are also present. Every step in the transformation from amphibolite to biotite hornblende gneiss can be observed. With increasing metamorphism, the amount of biotite and quartz increases and are associated with the development of porphyroblasts of garnet.

(c) Type II Brown hornblende amphibolite

Within the zone of the type I brown hornblende amphibolite, Type II amphibolites occur and strike comformably with that of the porphyroblastic plagioclase gneiss. The rocks are represented by a narrow, distinct belt in which migmatitic rocks with or without hypersthene and garnet are also associated (Pl. III). The migmatitic rock is granoblastic and resembles the other

migmatitic rocks of the Axial Zone with the exception that contains hypersthene and garnet. The porphyroblastic plagioclase gneiss on both flanks of the migmatite are intensely folded in a microscale with Type I amphibolite. Sillimanite is formed in the folded gneiss. The sheets of Type II brown hornblende amphibolite are not folded and are typically steeply inclined suggesting that they were intruded prior to migmatization but later than folding of the gneiss.

The Type II brown hornblende amphibolite is typically metablastic and consists essentially of brown to red brown hornblende and plagioclase (An_{60}-An_{40}), (Fig. 12). Numerous brecciated blocks of the amphibolite are enclosed within the migmatite of which the following types have been distinguished.

Cummingtonite-hypersthene-quartz-biotite amphibolite and Cummingtonite-hypersthene-biotite-gneiss (Fig. 13).

(d) Anthophyllite amphibolite

Along both flanks of migmatite and amphibolite described above, in the southern part of the belt, anthophyllite amphibolite is present (Fig. 14).

Further south, the axis of the migmatitic-amphibolite belt plunges beneath gneissic rocks, and discontinuous elongated outcrops of amphibolite occur along the axis for some 10km. This suggests that there is a genetic relationship betwen the hypersthene-garnet bearing migmatite, Type II brown hornblende amphibolite and the anthophyllite amphibolite.

In some areas the anthophyllite amphibolite has been converted to cordierite-cummingtonite bearing amphibolite by metamorphic replacement of original Type I brown hornblende amphibolite. The anthophyllite amphibolite and cordierite-cummingtonite amphibolite have been cited as examples of Fe-Mg metamsomatism associated with the genesis of cupfuriferrous pyrhotite deposits (Hunahashi, 1951). It is possible that the formation of anthophyllite and cordierite-cummingtonite amphibolite are related to the formation of a high temperature type of migmatite in the western part of the Axial Zone prior to the main phase of migmatite development.

(e) Biotite-hornblende gneiss

Biotite-hormblende gneiss forms a distinct belt some 1.5km wide and 40km long along the eastern margin of Type I brown hornblende amphibolite. The contact between the amphibolite and biotite-hornblende gneiss is gradational. Many relict lenses of Type I brown hornblende amphibolite are present in the biotite hornblende gneiss indicating that it was the parent rock (Fig. 9).

Plagioclase (zoned from $An_{43\text{-}30}$) is porphyroblastic. Hornblende, porphyroblastic-nematoblastic in habit, is pale green to pale greenish-brown in

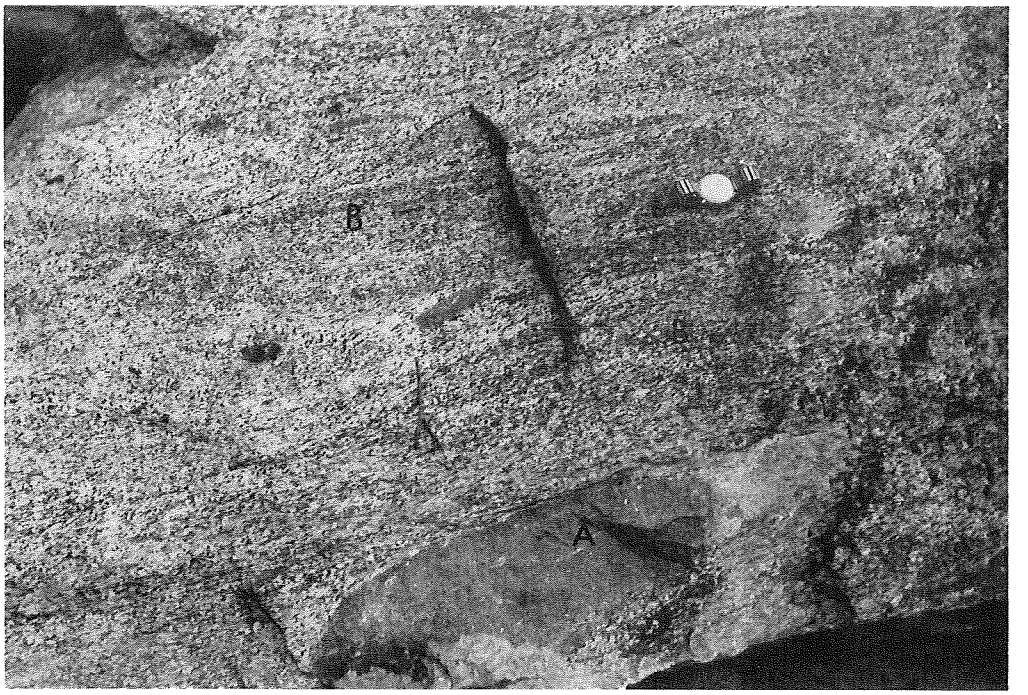

Fig. 9 Biotite-hornblende gneiss showing remnants of original brown hornblende amphibolite(A) and nebulitic schlieren of hornblende rich parts(B).

color and is elongated parallel to the schistosity plane which is sometimes obliquely cut by flakes of biotite. Quartz occurs in schlieren where it replaces plagioclase (Fig. 15).

(f) Schistose gabbro and pyroxene amphibolite

In the northern part of the metamorphic zone, another type of brown hornblende amphibolite, a schistose gabbro has been discriminated in the porphyroblastic plagioclase-biotite gneiss.

The schistose gabbro is similar in appearance to the Type I brown hornblende amphibolite described above (Fig. 16). Sheet-like bodies of schistose gabbro are typically associated with gneissose gabbro and crop out along the western margin of the gabbro. Remnants of schistose gabbro occur within the gneissose gabbro and have sharp or rapid gradational contacts with the enclosing rock (Fig. 17). Brecciation or agglomeration of the schistose gabbro presumably due to the intrusion of the gneissose gabbro is often seen.

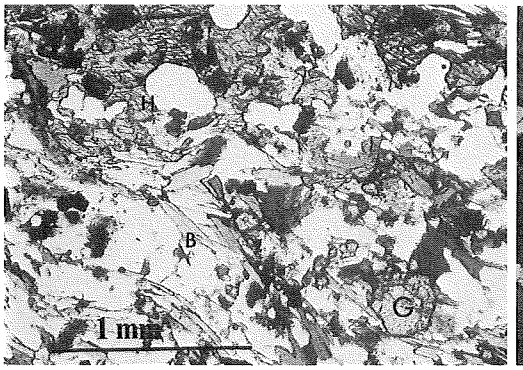

Fig. 10 Banded biotite amphibolite.
Amphibolitic part is shown in the upper part and leucocratic part in the lower part of the photo. Note the oblique trend of biotite flakes(B) with respect to the contact between the amphibolitic part and leucocratic part.

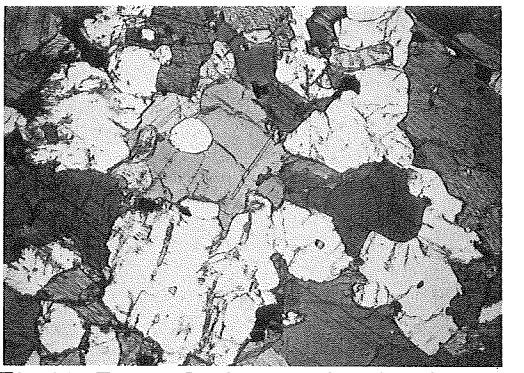

Fig. 11 Type I brown hornblende amphibolite.

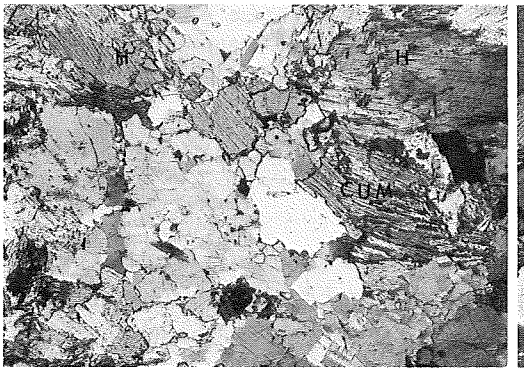

Fig. 12 Type II brown hornblende amphibolite.
Brown hornblende and cummingtonite are present.

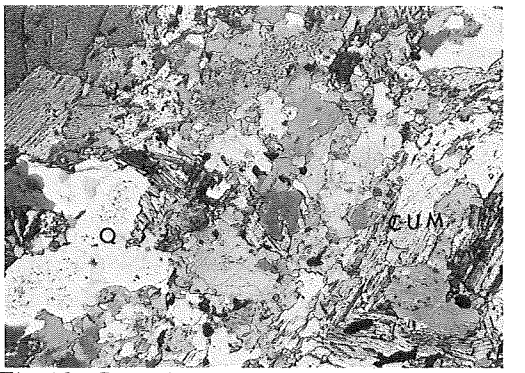

Fig. 13 Cummingtonite amphibolite.
Occurrence of hypersthene is not shown.
Note introduction of granular quartz.
Cum: Cummingtonite
Q: Quartz

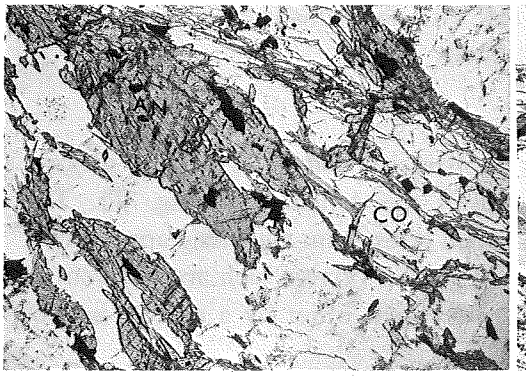

Fig. 14 Cordierite-anthophyllite amphibolite.
AN: Anthophyllite
Co: Cordierite

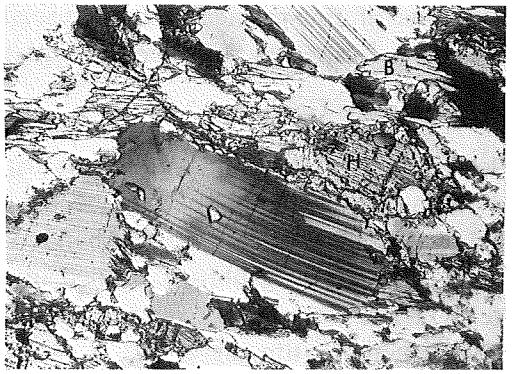

Fig. 15 Biotite-hornblende gneiss
H: Hornblende
B: Biotite

Fig. 16 Typical appearance of schistose gabbro composed of brown hornblende and plagioclase.

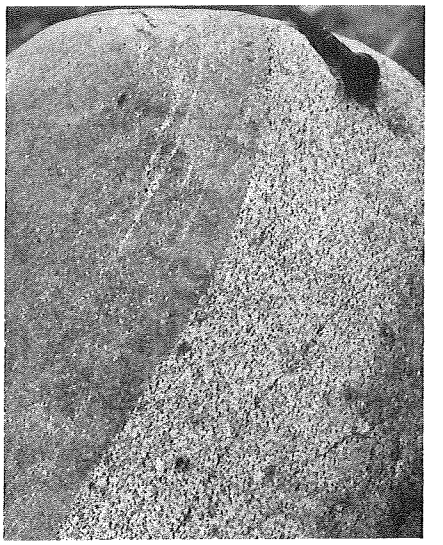

Fig. 17 Gneissose gabbro (right half) and noritized schistose gabbro. Note the coarser-grained seams in the schistose gabbro which parallel the gneissose gabbro contact.

The schistose gabbro has a nematoblastic to granulitic texture. The plagioclase (An_{65-55}) is a xenomorphic mosaic. Hornblende also has a mosaic or nematoblastic texture and is red brown or brown to greenish brown in color (Fig. 20, 21). Granular crystals of augite and hypersthene are commonly present.

Metamorphism caused by the intrusion of gneissose gabbro is demonstrated by the transformation of brown hornblende into rhombic pyroxene which is either coaxial with hornblende or forms poikiloblastic grains (Fig. 22). Small amounts of fine-grained norite associated with the schistose gabbro in places may have formed by this mode of replacement.

B. Gneissose Gabbro

In the northern Hidaka Mountains, an intrusive body of gneissose gabbro, 4–5km wide and 40km long occurs within the Axial Zone (Fig. 1). The gabbroic rocks are foliated and banded which gives them a gneissic appearance.

The gneissose gabbro is divided into two main types which are different in texture and composition and separated from each other by a narrow belt of hypersthene-biotite gneiss.

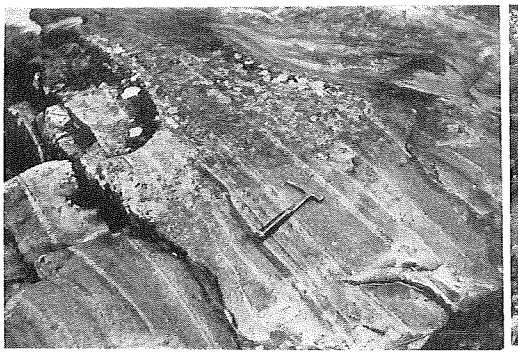

Fig. 18 Banded structure in Type I gneissose gabbro.

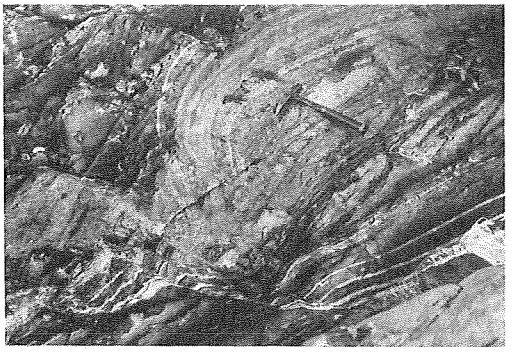

Fig. 19 Boudine of Type I gneissose olivine gabbro.
The marginal parts show distinct banding, parallel veining and foliation. The hammer rests on the unfoliated olivine gabbro core.

Each type of gneissose gabbro is composed of several varieties as follows

(a) Type I gneissose gabbro is composed of troctolite, olivine gabbro and norite.

(b) Type II gneissose gabbro is composed of olivine gabbro, gabbro, norite and biotite bearing gabbro.

(a) Type I Gneissose gabbro.

Gneissose gabbro is mainly composed of a coarse-grained, gneissose olivine gabbro, whose foliation strikes N-S or NNW-SSE and dips steeply to the east. The foliation is well developed along the western periphery and in the southern marginal part of the mass where it is separated into many arms penetrating schistose gabbro and biotite gneiss.

The gabbro is typically banded due to the parallel disposition of leucocratic and more mafic bands which may continue for some hundreds of metres (Fig. 18). In some localities trains of gabbro boundines free from foliations are enclosed in the gneissose gabbro (Fig. 19). A large mass of this type is centred in Mt. Pipairo. This kind of banding is of metamorphic origin and therefore entirely different from that commonly observed in the layered gabbros of the Mt. Poroshri Type, which is of cumulus origin (Miyashita, this volume). Nevertheless the western, or lower part of the gabbro consists of olivine gabbro and troctolite and the eastern, or upper part, consists of norite and gabbro.

Generally, the gneissose gabbro is felspathic and the mafic constituents do not exceed 40% in volume, even in rocks which contain olivine.

Gneissose olivine gabbro is exposed in the western part of the body and is some 3km wide and some 15km long. Foliation is strongly developed in the western part and becomes less conspicuous to the east.

In general, the rock is granulitic in texture and where strongly foliated has a cataclastic texture. Unzoned plagioclase (An_{75-60}) occurs as a xenomorphic mosaic. Olivine (Fo_{70}) is xenomorphic granular and usually has no reaction rims such as in the layered gabbro of Mt. Poroshiri. Monoclinic pyroxene (diallage) forms mosaic crystals (Fig. 24). Hypersthene has exsolution lamellae and is typically present in olivine poor gabbro.

Gneissose troctolite which is very rich in olivine (about 70%) crops out along the north-western periphery of the body. The texture is xenomorphic and probably is not of cumulus origin (Fig. 23).

To the east and towards the southern margin, the gneissose olivine gabbro gradually grades into gneissose norite. In many localities the gneissose norite shows evidence of intrusive emplacement into schistose gabbro and biotite gneiss as indicated by a lit-per-lit injection relation and brecciated contacts. In other localities gneissose norite is gradational into schistose gabbro and is characterized by hypersthene porphyroblasts, occuring as spots or streaks, replacing brown hornblende of schistose gabbro.

The gneissose norite is composed of mosaic granular plagioclase (An_{70-50}), prismatic to xenomorphic granular hypersthene and augite. Brown hornblende and minor biotite are accessory. Hypersthene has distinct exsolution lamellae. Augite usually occurs as individual crystals but some appear as rims around hypersthene (Fig. 25). Like the olivine gabbro the norite is banded with the parallel alignment of leucocratic norite bands of 1m to 10m wide. In places these bands are regularly developed but most dissappear within a hundred or so metres. Despite their obvious appearance in the field the individual bands have no significant difference in mineral composition, however, some are more coarser in grain size and may be accompanied by biotite and a minor amount of quartz.

(b) Type II gneissose gabbro

Type II gneissose gabbro is exposed in the south-eastern part of the body, and is separated from the Type I gneissose gabbro by a zone of biotite gneiss striking in a NNW direction from Mt. Esaoman-tottabetsu to the eastern slope of Mt. Pipairo. The gabbro is some 3km wide and 14km long and is separated into several elongated parts by the biotite gneiss. The Type II gneissose gabbro is not in direct contact with the Normal gabbro of the Eastern Zone but is

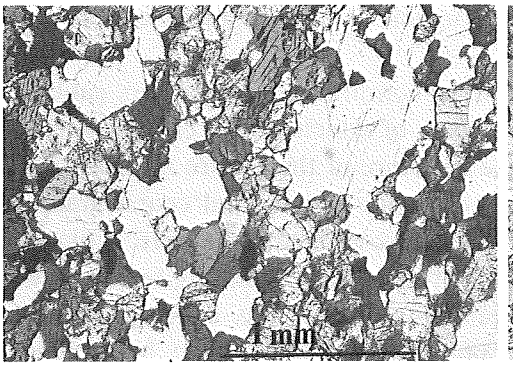

Fig. 20 Pyroxene bearing schistose gabbro showing granulite texture.

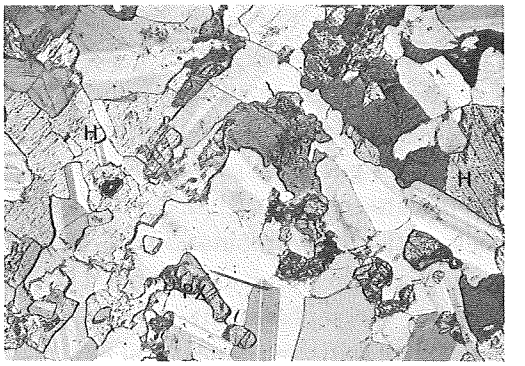

Fig. 21 Schistose gabbro with ophitic texture.
Px: Pyroxene, H: Brown hornblende (Partly crossed nicols)

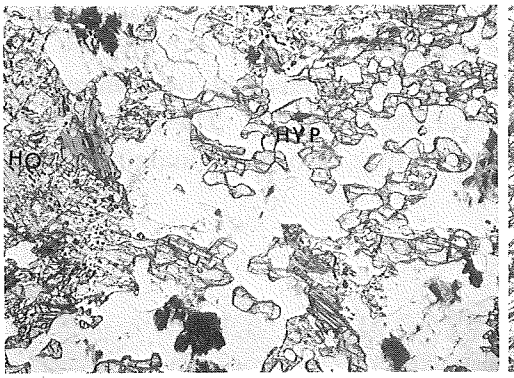

Fig. 22 Pyroxenized schistose gabbro showing poikiloblastic hypersthene (Hyp) and bleached and corroded brown hornblende(Ho).

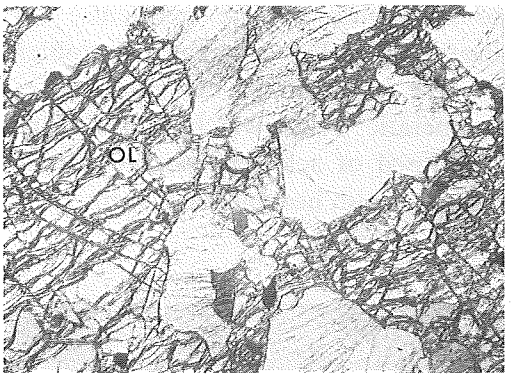

Fig. 23 Troctolite of Type I gneissose gabbro.

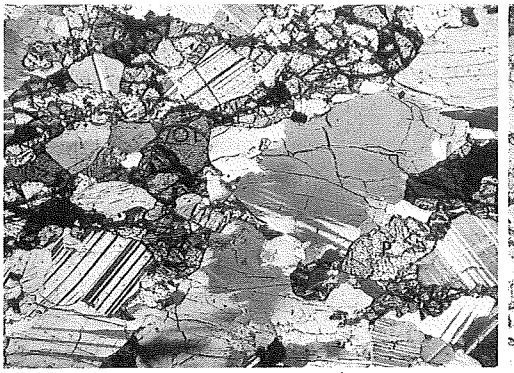

Fig. 24 Olivine gabbro of Type I gneissose gabbro showing xenomorphic granular texture. Ol: Olivine, P: Clinopyroxene (Partly crossed nicols)

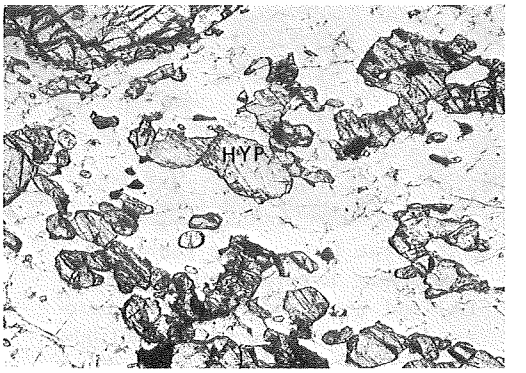

Fig. 25 Norite of Type I gneissose gabbro.
Hyp: Hypersthene

separated from the latter by another major belt of biotite gneiss east of the gneissose gabbro body.

The rocks of the Type II gneissose gabbro comprise olivine gabbro, gabbro, norite and biotite bearing gabbro the foliation of which is weaker than that of the Type I gneissose gabbro. However, the structure of the gabbro is dominated by the alternation of leucocratic bands and of fine-grained and coarse-grained rock facies or combination of both. The coarse-grained bands are typically gradational to massive, unbanded rocks. Texturally some banding seems to be formed by replacement of the fine-grained rock by the development of porphyroblastic plagioclase. The fine-grained gabbro and norite have xenomorphic granular to subophitic texture. The plagioclase ranges in composition from $An_{60\text{-}50}$. In the fine-grained rocks elongation of plagioclase shows a subparallel arrangement with the banding. Augite and hypersthene are granular to subophitic and are frequently enclosed by poikilitic brown hornblende. Biotite generally accompanies hornblende (Fig. 26).

The foliation of the gneissose gabbro is often traversed by swarms of leucocratic veins which follow tension cracks (Fig. 27). These veins are composed of acidic plagioclase, quartz and biotite. Along the margins of the veins greenish hornblende is formed.

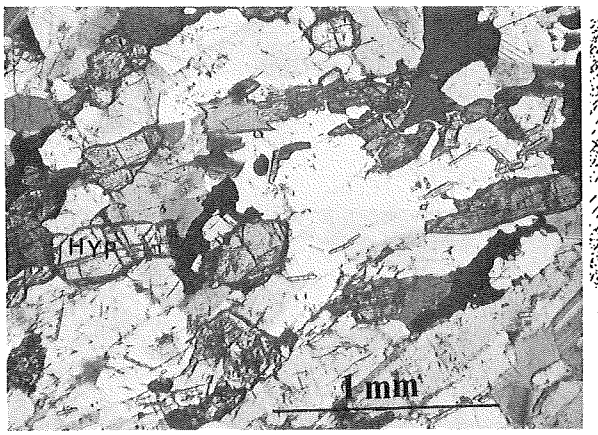

Fig. 26 Type II Gneissose gabbro with plagioclase, hypersthene(Hyp), augite (A) and hornblende(H). Photomicrograph of the leucocratic band(right figure). The dark band rock shows similar texture and composition. (Partly crossed nicols)

Fig. 27 Banding in Type II gneissose gabbro and cross cutting leucocratic veins.

(c) Primary cumulate rock

At Mt. Kita-tottabetsu large blocks (up to 1km in diameter) of primary layered heteradcumulate troctolite and olivine gabbro, the same as those of the Poroshiri mass, are enclosed and disrupted by fine-medium grained noritic gabbro with an ophitic texture. At the margin of the mass the noritic gabbro become gneissose and grades into a gneissose hornblende gabbro, (R. Grapes, personal communication).

(3) The Eastern Zone

The eastern Zone of the Hidaka Metamorphic Belt crops out to the east of the Axial Zone and comprises gabbro, diorite, granite and associated metasedimentary rocks of the Hidaka Supergroup (Fig. 1).

A. Normal Gabbro

Normal gabbro occurs as discordant to sub-discordant intrusive masses which are exposed in the areas of Karikachi Pass, Mt. Memuro, along the middle part of the Tottabetsu River in the northern part of the metamorphic belt, and in the Horoman area, Mt. Notsuka and Oshirabetsu district in the southern part of the metamorphic belt (Pl. II and Pl. III).

Each intrusive mass comprises a heterogeneous complex of olivine gabbro, gabbro (hyperite), norite, hornblende gabbro and diorite.

In the Tottabetsu plutonic mass, the western side of the intrusive is basic and gradually become less basic to the east.

The Opirar-kaomap mass in the Horoman area consists of two elongated exposures separated by SSE to NNW trending gneiss septa. The western part is composed of olivine gabbro and pyroxene gabbro, while eastern part has the composition of a hornblende gabbro.

The occurrence of each type in each intrusive mass can be tabulated as follows:

	1	2	3	4	5	6	7
Olivine Gabbro	○	○	○		○		○
Pyroxene Gabbro	○	○	○		○	○	○
Norite	○	○	○		○	○	
Hornblende Gabbro	○	○	○	○	○	○	○
Diorite	○	○			○		

1: Oshirabetsu 2: Horoman 3: Mt. Notsuka 4: Nakanokawa River
5: Tottabetsu River 6: Mt. Memuro 7: Karikachi Pass

(a) Olivine gabbro

The olivine gabbro is generally coarse-grained and the structure can be determined by the development of weak banding. Layering of cumulus origin is present in the gabbros exposed in the Oshirabetsu and Mt. Notsuka areas.

The rocks are typically composed of domains showing a considerable variation in grain size and texture. Each domain is very irregular in form but typically occupies 1–2cm in diameter. Some domains have a xenomorphic-hypautomorphic granular texture of olivine (around 0.5mm in diameter) and plagioclase ($An_{75\text{-}60}$, 1–2mm in the longest axis). Such domains are termed "domains of granular mineral association".

Many of the granular domains are surrounded by patches of idiomorphic plagioclase ($An_{80\text{-}60}$) and poikilitic clinopyroxene with ophitic texture ("domain of ophitic mineral association"). There is a considerable variation in the relative amount of these two kinds of domain (Fig. 28).

(b) Pyroxene Gabbro

Pyroxene gabbro shows two different modes of occurrence. One type is a coarse-grained, homogeneous rock which is usually associated with the olivine gabbro and is gradational into the olivine gabbro. This pyroxene gabbro has a hypautomorphic granular texture with subidiomorphic plagioclass (zoned from

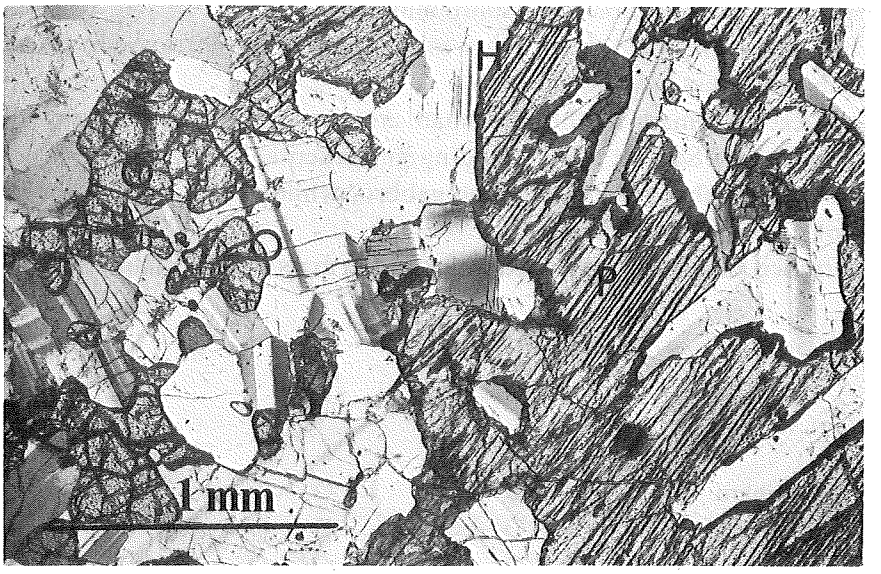

Fig. 28 Two domains in olivine gabbro.
Domain of granular mineral association with olivine(O) and plagioclase (left side) and domain of ophitic mineral association with plagioclase and augite(P) partly replaced by brown hornblende(H). (right side), (partly crossed nicols)

An_{85-55}) and interstitial xenomorphic clinopyroxene showing exsolution lamellae on (001). A considerable amount of hypersthene is present and forms subidiomorphic crystals.

The other type of pyroxene gabbro is associated with hornblende gabbro and forms large (500m–1km or more) lenticular bodies which are cut by the hornblende gabbro. These pyroxene gabbros are fine-grained with a diabasic to intersertal texture (Fig. 32). Plagioclase (zoned from An_{75-50}) occurs as slender lath-shaped crystals and is accompanied by subidiomorphic hypersthene. Along the contact with the hornblende gabbro, the grain size of the pyroxene gabbro become coarser. Large crystals of plagioclase (up to 5mm in length) are often observed near this contact and are elongated parallel to the contact (Fig. 29). Granular and ophitic domains, the same as in the olivine gabbro, also occur in the pyroxene gabbro (Fig. 33).

(c) Hornblende gabbro

Hornblende gabbro is a common constituent of normal gabbro bodies. Along the Tottabetsu River, the hornblende gabbro is typically exposed in the eastern portion of the igneous body and is associated with diorite along the eastern most marginal part.

The hornblende gabbro has two varieties differing in grain size and in texture (Fig. 34 and 35). The fine-grained hornblende gabbro or diabasic hornblende gabbro is homogeneous and has ophitic to subophitic texture.

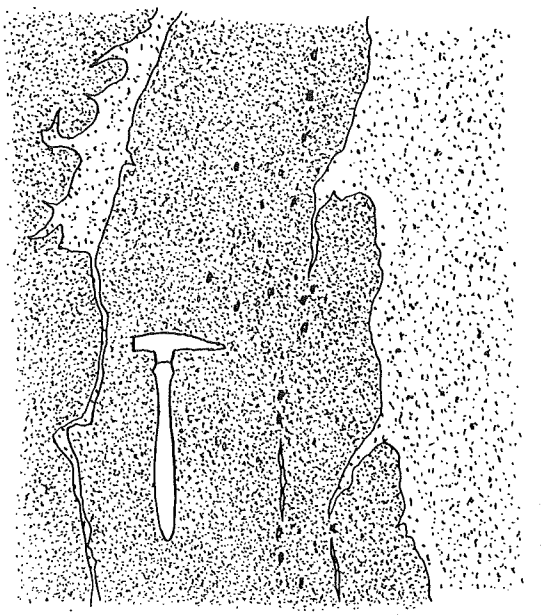

Fig. 29 Field relationship between fine-grained pyroxene gabbro and coarse-grained pyroxene or hornblende gabbro (see text for explanation).

Lath-shaped plagiocalase (zoned from An_{70-50}) and subhedral hornblende are the chief constituents and are accompanied by accessary amounts of biotite and Fe ore. Quartz is rarely present.

Associated with the fine-grained hornblende gabbro, is a medium to coarse-grained hornblende gabbro which forms irregular bodies of different size (from several meters to 1km). In some areas banding (on a meter scale) occurs between the hornblende gabbro and the fine-grained gabbro (Fig. 30).

The medium-grained hornblende gabbro has a hypautomorphic granular texture. Plagioclase (zoned from An_{60-50}) is subidiomorphic, typically between 3–6mm in length. Hornblende is greenish brown to deep brown in color and occurs interstitially to plagioclase. Relicts of augite may be present within hornblende. The coarse-grained hornblende gabbro occurs as spots, lenses or bands, which are commonly developed near the fine-grained gabbro or arround inclusions of fine gabbro within the medium-grained hornblende gabbro. The coarse-grained rock is hypautomorphic granular in texture and has the same mineralogy as the medium-grained variety.

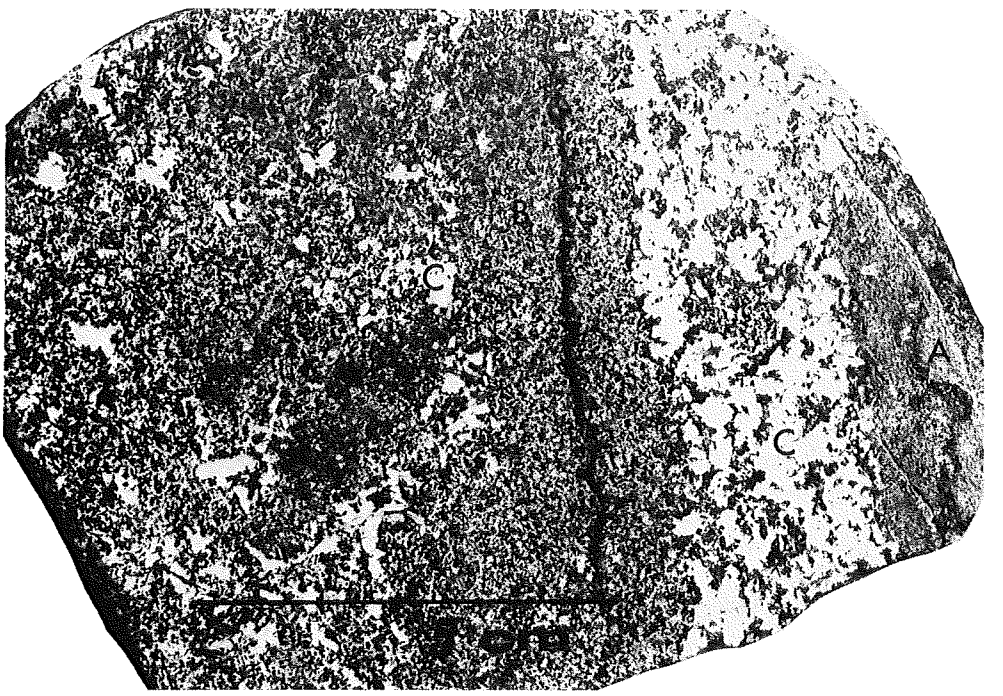

Fig. 30 Megascopic characteristies of the mottled hornblende gabbro.
A: diabasic part cfr. Fig. 34
B: medium-grained part cfr. Fig. 35
C: the coarse-grained part cfr. Fig. 36

(d) Diorite

With increasing amounts of biotite and quartz the coarse-grained hornblende gabbro is gradational into diorite (Fig. 36). In the Tottabetsu area, diorite is exposed along the Pirikapetan River and forms schlieren or irregular bodies in which zoisite and chlorite occur as late stage products. In the Oshirabetsu area, the diorite is formed by replacement of gabbroic rock due to an introduction of granitic material.

Some parts of the norite contain orthoclase and quartz together with plagioclase, hypersthene, augite, hornblende and biotite. The rocks are coarse-grained and have irregular pegmatoid segregations which are characterized by porphyroblastic quartz up to 5cm or more in diameter. The chemical composition of this rock indicates that it is a diorite despite of the occurrence of pyroxene (Tab. II No. 81). The frequent occurrence of graphite associated with the pegmatoid segregations suggests a probable migmatitic origin.

In this repect the diorite exposed in the Mt. Notsuka area is of particular interest. Here, an intrusive body of hornblende gabbro has been migmatized to form a heterogeneous dioritic rock which contains abundant patches of the original rock being enclosed by quartz-biotite diorite indicating the diverse origin of such rocks in the Hidaka Metamorphic Belt.

(e) Layered gabbro of Ame-yama

Layered gabbro is exposed in the Ame-yama area (A in Pl. II) as a small hill in the Tokachi Plain. The hill is situated 30km east of the Hidaka Metamorphic Belt and is an outlier surrounded by Quarternary deposits.

The layering of this gabbro body is rather weak and although no distinct layer can be observed, the gabbro seems to be titled gently to the north. The gabbroic rocks are excellent examples of unmetamorphosed cumulate rocks characterized by orthocumulate (cumulus olivine + plagioclase); adcumulate (cumulus olivine + clinopyroxene + plagioclase) and heteradcumulate (cumulus olivine + intercumulus clinopyroxene) textures (Fig. 37). Near the top of the exposure, cumulus plagioclase shows well developed igneous lamination.

B. Minor Basic Intrusives

(a) Diabase dikes. Basic dikes are common in the southern part of the Hidaka Metamorphic Belt and intrude rocks of the Axial Zone and Eastern Zone. The dikes are generally 10 to 1m in width, have a sharp contact with the host rocks, and occur as parallel swarms. The dikes are representative of several intrusive episodes because some diabases have been metamorphosed to diabasic hornfelses while other diabase dikes intruded near the metadiabase dikes (which may belong to the earliest intrusive phase) intrude porphyroblastic

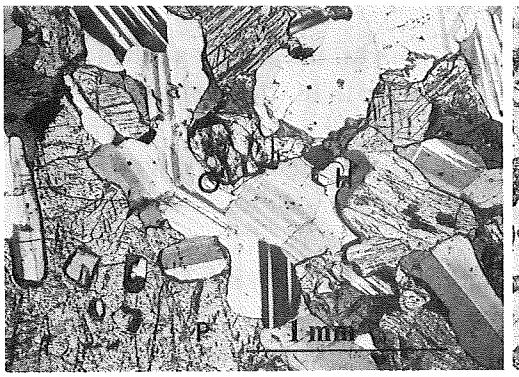

Fig. 31 Olivine gabbro with clinopyroxene(P), plagioclase and brown hornblende(H).
(partly crossed nicols)

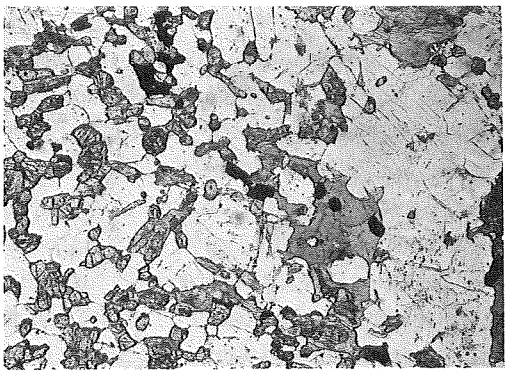

Fig. 32 Fine-grained pyroxene gabbro with coarse-grained plagioclase associated with xenomorphic granular brown hornblende(H).
(open nicol)

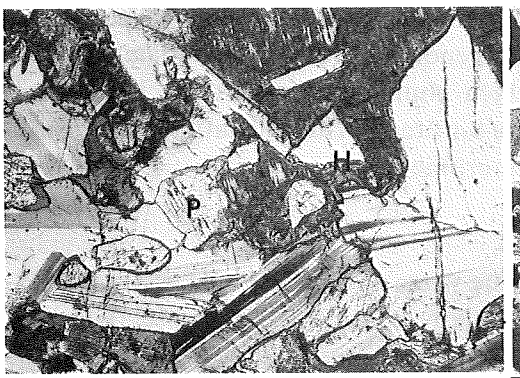

Fig. 33 Mottled part of pyroxene gabbro with clinopyroxene(P) and brown hornblende(H).
(partly crossed nicols)

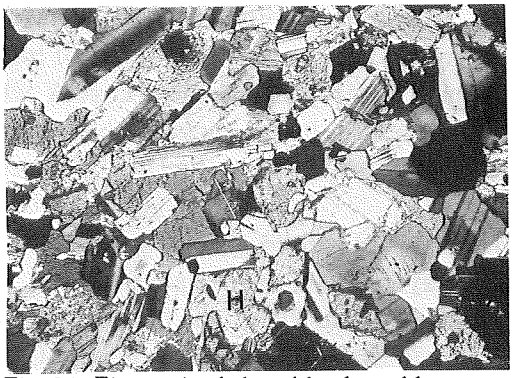

Fig. 34 Fine-grained hornblende gabbro with idiomorphic granular plagioclase and ophitic hornblende(H).
(partly crossed nicols)

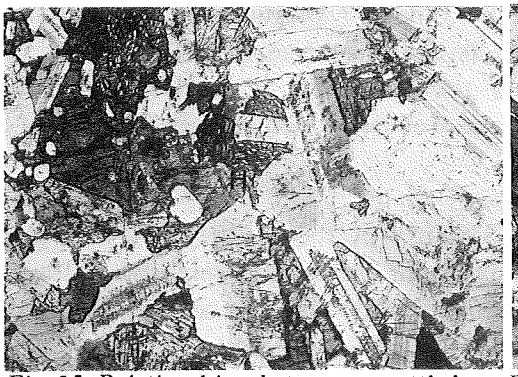

Fig. 35 Relationship between mottled hornblende gabbro and fine-grained rock.
(partly crossed nicols)

Fig. 36 Diorite occurring as spots within hornblende gabbro with plagioclase, brownish green hornblende(H) and quartz(Q).
(partly crossed nicols)

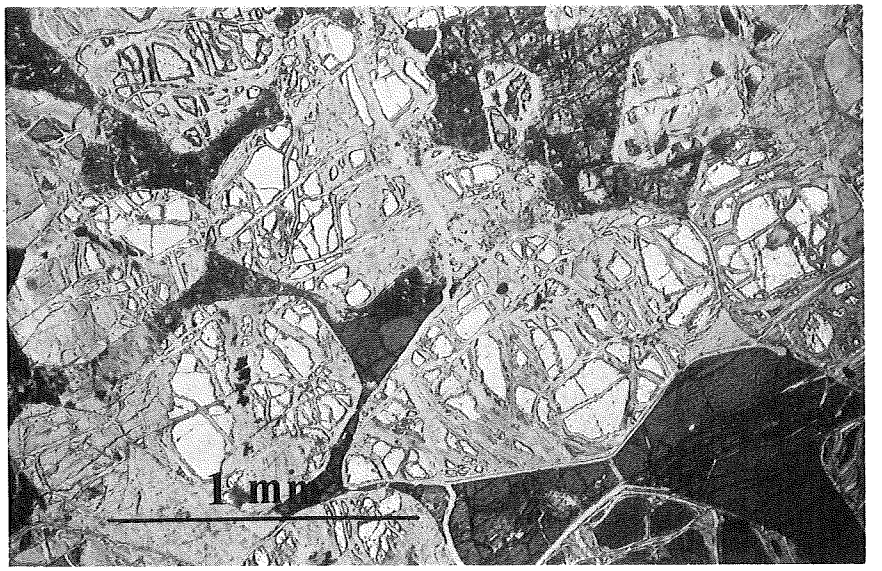

Fig. 37 Cumulus olivine and intercumulus clinopyroxene rock of Ame-yama layered gabbro. The texture is heteradcumulate.

plagioclase-biotite gneiss and strike obliquely to the general strike of the host gneiss. They have been migmatized in parts. Other metamorphosed dikes are well exposed in the Mt. Notsuka area in the southern part of the metamorphic belt. Some of these diabase dikes are composite and have a felspathic inner zone which is bordered by diabasic margins. They cut across all rock types, including granite, and form a swarm trending in a N-S direction.

Within the granite body, the dikes intrude along the planes of the major cross joints, indicating that their formation was later than the consolidation of the granite. However, some diabase dikes have been metamorphosed and partially mobilized within some of the migmatitic rocks. Fig. 38 illustrates such a phenomena. The form of the diabase dikes remains unchanged in the cordierite bearing migmatite but are disrupted and partially mobilized* within coarse-grained leucocratic migmatite bands.

(b) Metaporphyrite and amphibolite dikes within ultramafic rocks: Metaporphyrite and amphibolite dikes occur within the ultramafic rocks near Mt. Tottabetsu. Metaporphyrite refers to thermally metamorphosed rocks which still preserves initial porphyrite textures. Amphibolite occurs as disrupted dikes within perioditite. Some of the dikes contain xenoblastic plagioclase which resembles that in the Type I brown hornblende amphibolite or schistose gabbro. However, the ultramafic rocks and brown hornblende

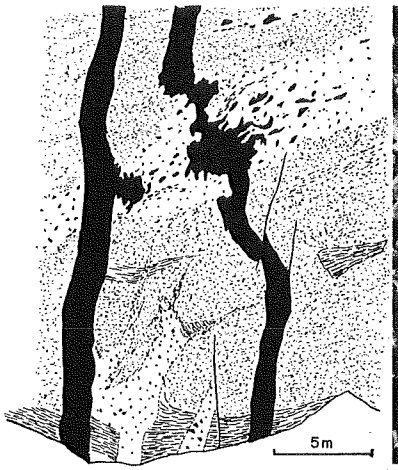

Fig. 38 Occurrence of partly migmatized (mochiized,* see text) diabase porphyrite dike cutting cordierite bearing biotite migmatite.
The dikes are transformed into biotite amphibolite in the migmatized part (upper stream of the Niobetsu Riber).

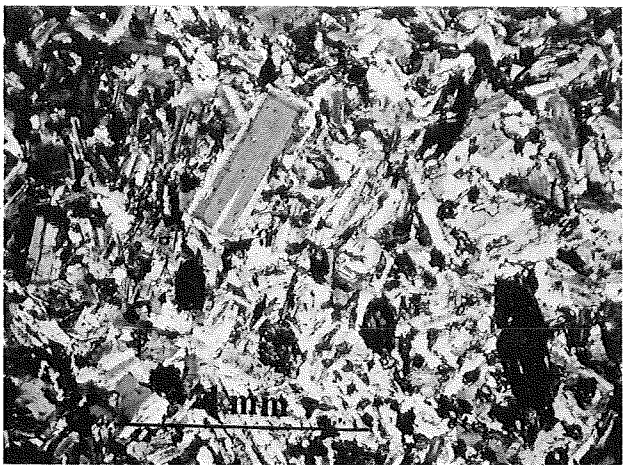

Fig. 39 Diabase porphyrite
Same dike rock as that shown in Fig. 38

amphibolite belong to entirely different tectonic units and there is no direct evidence which indicates the source of the metaporphyrite and amphibolite dike magmas.

(4) Septa Rocks

As mentioned above, the gabbroic rocks of the Western, Axial and Eastern Zone of the Hidaka Metamorphic Belt are separated into several characteristic groups by narrow belts of septa rocks which have a considerable variation in composition. In the Poroshiri Plutonic Complex where all types of Hidaka gabbro are developed, the septa rocks are well exposed.
Three types of septa rocks have been distinguished:

(a) Type I Septa hypersthene-cordierite-garnet-biotite gneiss etc.
(b) Type II Septa fine-grained hypersthene-biotite gneiss.
(c) Type III Septa coarse-grained hypersthene-cordierite bearing biotite hornfels.

(a) Type I Septa

The original rocks of Type I septa chiefly consist of porphyroblastic-plagioclase-biotite gneiss. The gneiss is highly foliated and spotted by the occurrence

* The author considers that a good term to describe such a process is "Mochiization" in analogy with process of Mochi making in Japan in which Mochi (rice paste) when heated, become partially mobilized.

of porphyroblasts of plagioclase (An_{40-30}; 3–2mm in diameter). Fine-grained quartz and plagioclase associated with flakes of light brown biotite occur interstitially to the plagioclase porphyroblasts. Garnet porphyroblasts are rarely found.

Within the septa, the gneiss is intensely metamorphosed to form a hypersthene-cordierite-garnet-biotite-plagioclase-quartz assemblage. The plagioclase porphyroblasts are recrystallized to form a medium to fine-grained mosaic. The metamorphosed rocks of the septa are as follows:

Biotite-hypersthene-gneiss (Fig. 40)
Garnet-cordierite-hypersthene-biotite gneiss (Fig. 41)
Spinel-cordierite-hypersthene-biotite gneiss

(b) Type II Septa

The boundary between the two types of the gneissose gabbro described above, is defined by rocks of Type II septa which have the mineral composition of hypersthene-biotite-plagioclase-quartz. In comparison with the Type I septa rocks, the grain-size of the Type II septa is finer. Most of the septa are characterized by abundant inclusions of calc-silicate nodules the mineral assemblage of which is diopside, plagioclase and quartz which are surrounded by a fine-grained rim of hornblende, biotite, quartz and plagioclase (Fig. 42).

(c) Type III Septa

Calc-silicate nodules are also common in rocks of Type III septa which occur within the bodies of normal gabbro. Type III septa occur as comparatively narrow bands up to 50m wide and are more or less confined with each of the normal gabbro bodies. The gabbro adjacent to the septa is noritic in composition and is fine-grained suggesting rapid cooling.

The rocks of Type III septa are biotite hornfels characterized by poikiloblastic biotite (Fig. 43). Minute grains of hypersthene and cordierite are present in the middle part of the septa and increase in amount towards the margins. In some areas granitic segregates are formed. It is interesting to note here that some of the calcareous nodules in the Type III septa contain anglar grains of clastic quartz suggesting that their orgin may be sedimentary.

Evolution of the Basic Plutonic Rocks in the Hidaka Metamorphic Belt

Intrusion of basic rock occured successively throughout the metamorphic history of the Hidaka Metamorphic Belt. A schematic diagram of the succession of intrusion is illustrated in Pl. I and Fig. 44.

Two fundamentally different basic rock stems exist.

(A) Ultramafic rocks and primary cumulate layered gabbro rocks (i.e., at Mt.

Poroshiri, Mt. Kita-tottabetsu and Ame-yama etc.) including their metamorphosed equivalents (metagabbro-gabbroic amphibolite-green hornblende amphibolite-epidote amphibolite).

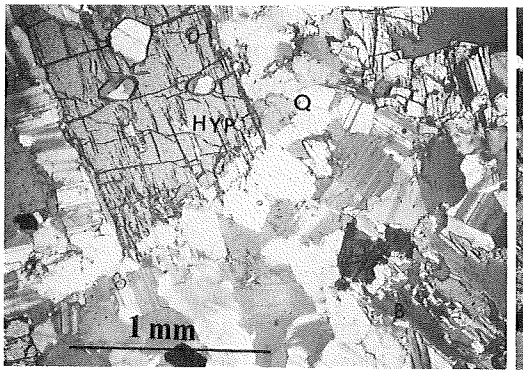

Fig. 40 Type I septa rock with biotite (B), hypersthene(HYP), quartz(Q) and plagioclase. Idioblastic development of hypersthene is characteristic. (Partly crossed nicols)

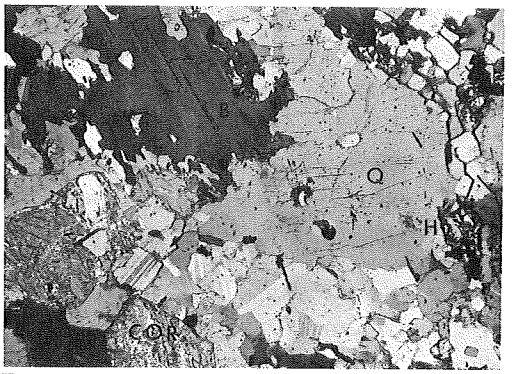

Fig. 41 Type I septa rock with biotite (B), hypersthene(H), cordierite(Cor), quartz(Q) and plagioclase. (Partly crossed nicols)

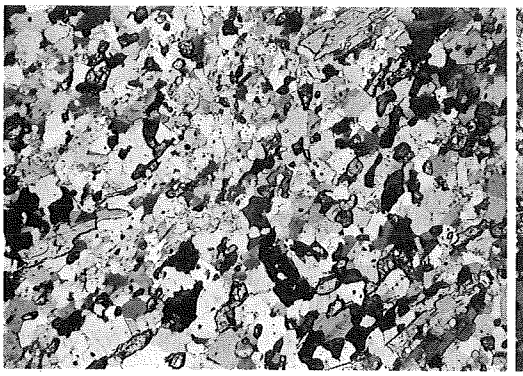

Fig. 42 Type II septa rock with biotite, cordierite, hypersthene, quartz and plagioclase. (Partly crossed nicols)

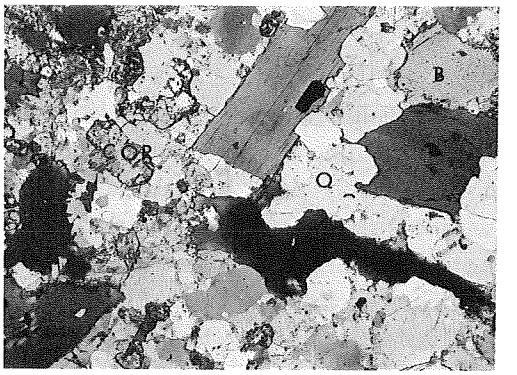

Fig. 43 Type III septa rock consisting of cordierite(Cor), biotite(B), quartz(Q) and plagioclase with or without hypersthene. (Partly crossed nicols)

(B) Syn-kinematic gneissose olivine and pyroxene gabbro, norite and troctolite and post-kinematic normal gabbro, including olivine gabbro, pyroxene gabbro, hornblende gabbro and diorite.

Ultramafic and gabbroic rocks of Type I stem have been emplaced tectonically while those of Type II were intruded in a liquid or semi-liquid state prior to the end of the metamorphic episode of the Hidaka Orogeny.

(A) Gabbroic Rocks of the Stem I

The preservation of primary layered cumulate rocks indicates stable conditions of crystallization and solidification prior to disruption and upward tectonic emplacement. Emplacement of gabbros of the Type I stem is indicated by the upward and westward thrusting in the form of sliced sheets, along the margin of the metamorphic belt. This resulted in the dynamic metamorphism of the gabbroic rocks to form the metagabbro–gabbroic amphibolite–green hornblende amphibolite–epidote amphibolite series that is exposed in the Western Zone of the metamorphic belt and representing the so-called "alpine root zone type of intrusion".

The time of emplacement of the stem I gabbroic rocks cannot be established with certainty. However, the final movement of uplift of the metamorphic belt occured in Post-Miocene or Pliocene times, because Miocene deposits located very near to the Western Boundary Thrust have been extensively block faulted presumably by the uplift movement of the metamorphic belt.

The metamorphic grade of the amphibolite in the Western Zone is generally higher towards the eastern margin although shearing is much more intense towards the western margin. This difference is indicative of both the westward thrusting of the rocks and to the heating effects of the gneissic gabbros of the Axial Zone bordering the eastern amphibolite.

Ultramafic rocks along the western margin of the Western Zone are commonly sheared, although, in places original structures such as layering between dunite, harzburgite and plagioclase Lherzolite is preserved. It is suggested here, although further study is needed, that the ultramafics form a continuous series with the layered gabbroic rocks of the Type I stem.

(B) Gabbroic rocks of the Stem II

Time relations of basic igneous activity in the Axial and Eastern Belt are difficult to identify precisely because the stages of intrusion ranged over a long period of time and there were repeated interactions between metamorphism, magmatitization and basic intrusion.

The earliest intrusion of basic rocks in these zones occured along the western margin of the porphyroblastic plagioclase-biotite gneiss that had already been formed during the initial stages of metamorphism (Pl. I). The gneiss was probably still at a high temperature when intrusion and concomitant metamorphism of diabase and Type I brown hornblende amphibolite took place. The uniformity in mineralogy of the brown hornblende amphibolite throughout in the Hidaka Metamorphic Belt and their restricted occurrence within this type of gneiss supports this conclusion.

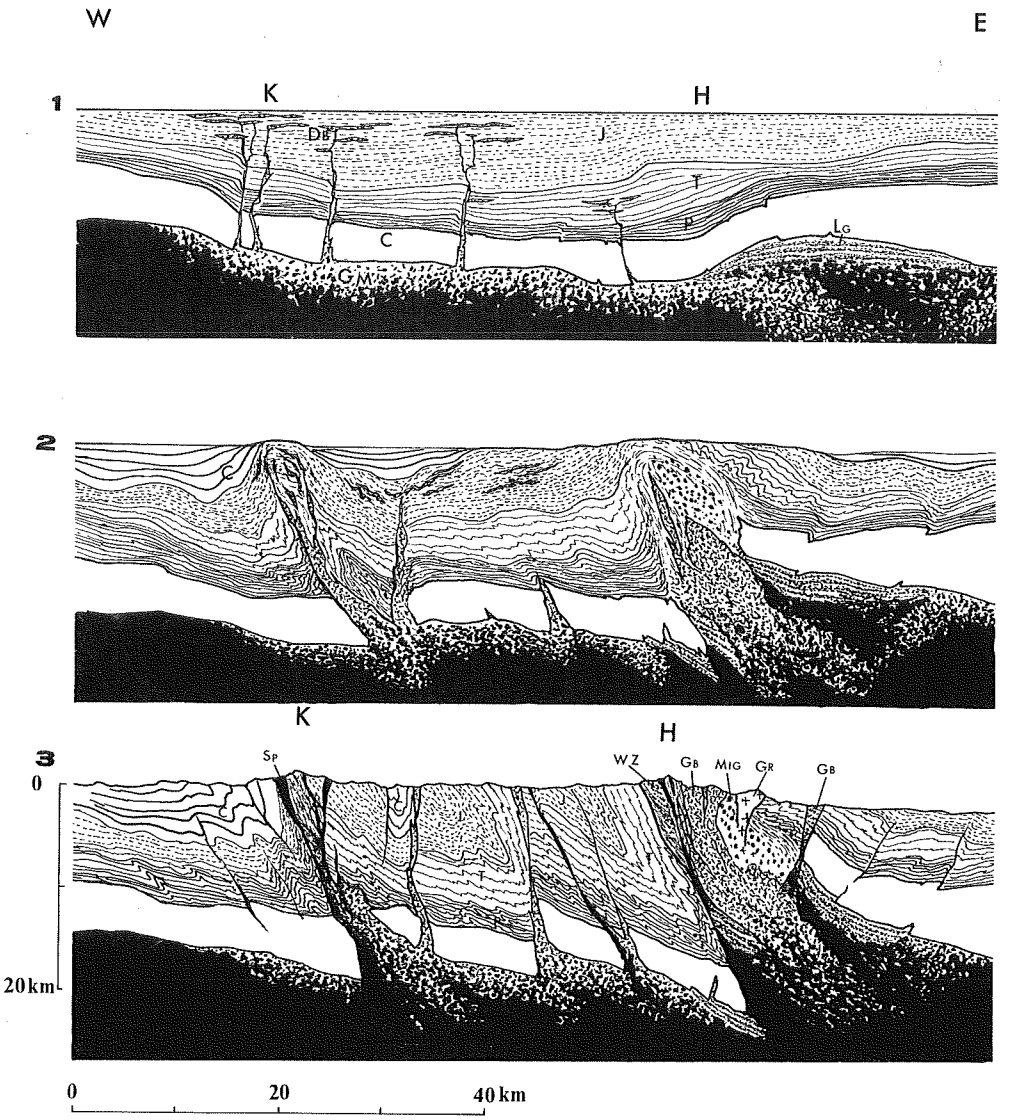

Fig. 44 Geologic section across the Hidaka Metamorphic Belt and the Kamuikotan Belt. (Revised from Hunahashi and Hashimoto, 1965)

1- H: Hidaka Metamorphic Belt K: Kamuikotan Belt DB: Diabase LG: Layered basic-ultrabasic complex J: Jurassic T: Triassic P: Paleozoic C: Crust GM: Gabbroic magma formed by partial melting of mantle (End of Jurassic time)

2- M: Migmatite was forming. (End of Cretaceous)

3- WZ: The western Zone GB: Gabbros MIG: Migmatite GR: Granite SP: Serpentinite

In the central and southern parts of the Hidaka Metamorphic Belt, high temperature migmatitization occuring along the western margin of the porphyroblastic plagioclase-biotite gneiss belt was closely preceeded by the formation of Type II brown hornblende amphibolite which was disrupted by the migmatite. The Type I brown hornblende amphibolite has been intensely folded together with the enclosing gneiss during formation of the migmatite.

The intrusion and simultaneous metamorphism of Type I and Type II brown hornblende amphibolite was followed by the intrusion of gabbroic rocks in a partly liquid state to form the Type I gneissose gabbro. The formation of the Type I gneissose gabbro was preceded by that of the schistose gabbro which formed elongated bodies along the western margin of the latter. The schistose gabbro was probably diabasic in composition at the time of injection, and was metamorphosed during consolidation to form a schistose gabbro similar in composition to that of the brown hornblende amphibolite. The presence of pyroxene coexisting stably with hornblende in some of the schistose gabbros suggests that these rocks solidified under a higher temperature than that of the brown hornblende amphibolite.

The gradual compositional change of the gneissose gabbro from olivine gabbro to norite towards the east suggests, that successive intrusion and petrological younging from west to east occured over a short interval of time. Partial granulation and mechanical deformation of the gneissose gabbro suggests cooling under stress. Relictic boundines of olivine gabbro in the Mt. Pipairo area which still retain relatively underformed igneous textures, may be representative of the original form of the Type I gneissose gabbro and therefore indicates that, unlike the rocks of the Type I gabbro stem, those of stem II were probably not of cumulus origin. Rather these rocks were probably injected in a mushy state and solidified under tectonic stress at high temperature as indicated by their gneissic structure. Previously emplaced schistose gabbro and septa rocks were recrystallized by and incorporated into the gneissose gabbro to form norite and hypersthene-garnet-cordierite-spinel rocks etc.

Prolonged and successive intrusion of the gneissose gabbro probably resulted in the development of the foliated gabbro of the Type II in the south-eastern part of the Type I gneissose gabbro body. The chief differences between the Type II and Type I gneissose gabbro are in the following:

(a) Type II gneissose gabbro is heterogeneous in grain size. It has strongly developed banding between coarse-grained and fine-grained gabbro in which the former also intrudes the latter.

(b) Olivine gabbro is rare in the Type II gneissose gabbro but is a major rock type of the Type I gneissose gabbro.

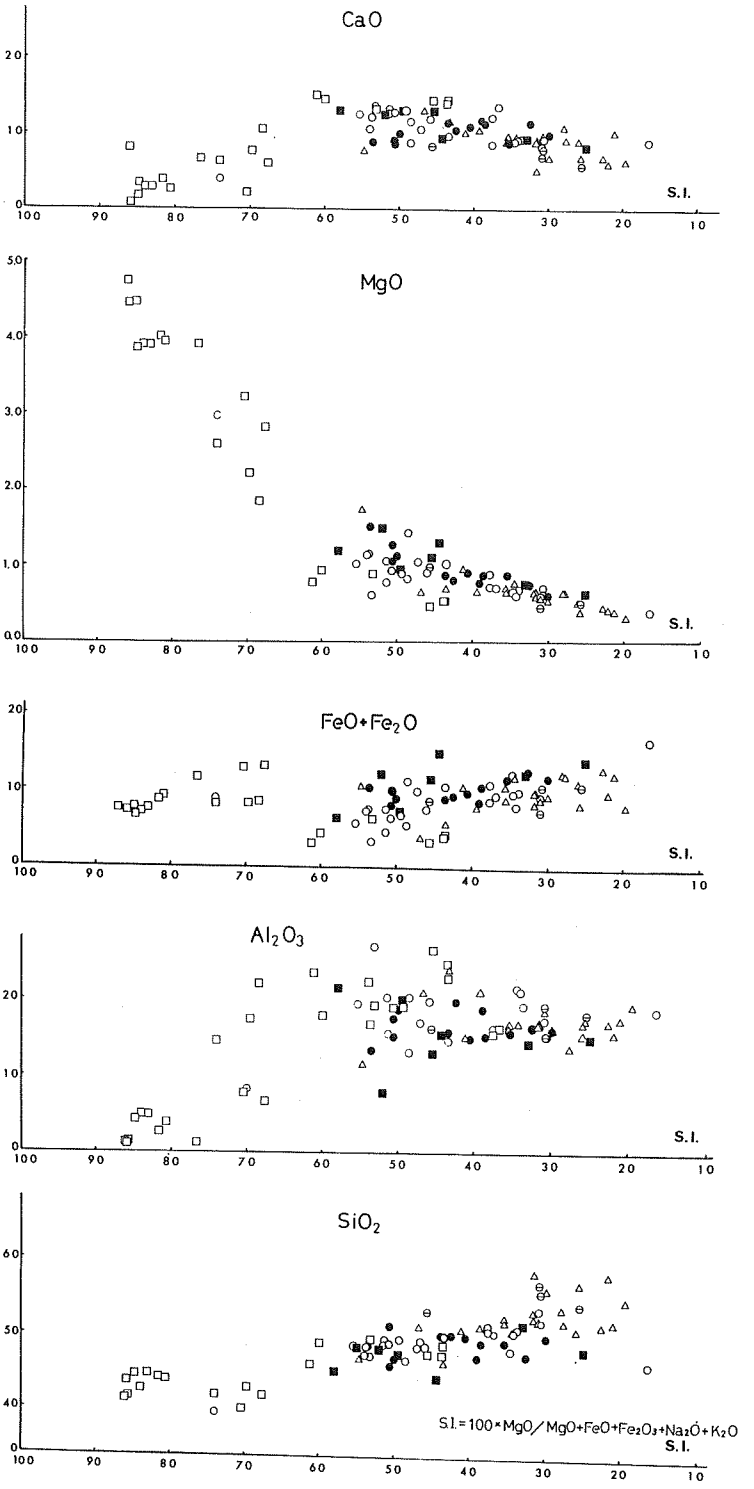
CaO
MgO
FeO+Fe2O
Al2O3
SiO2
S.I.
S.I.=100*MgO/MgO+FeO+Fe2O3+Na2O+K2O

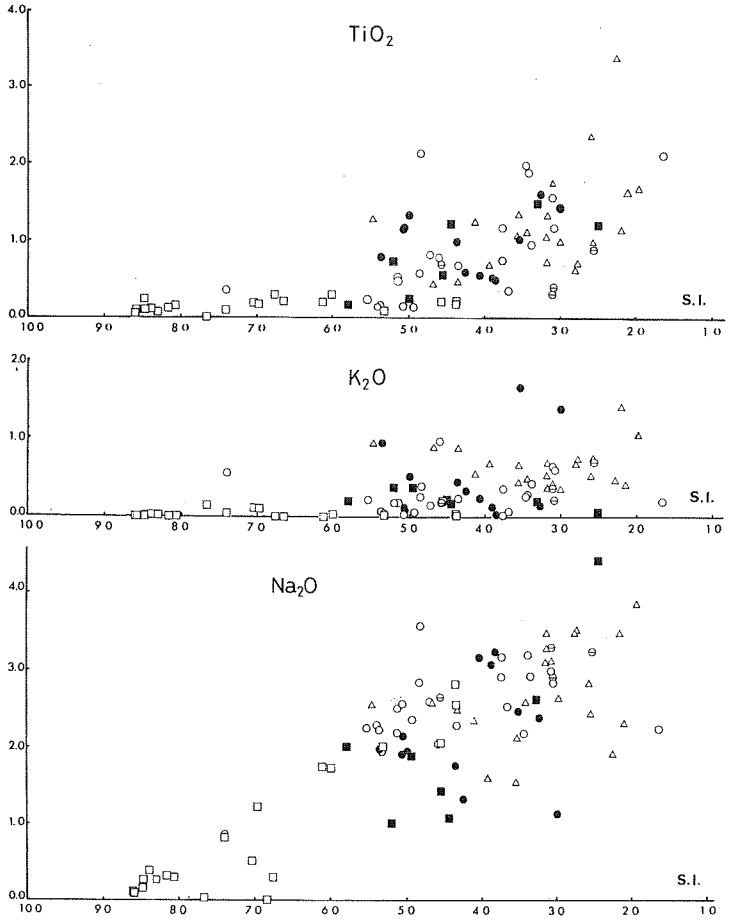

Fig. 45 S.I. Variation diagrams for the Hidaka basic rocks.
open squares: Ultrabasics, layered gabbro and metagabbro, rocks of the Western Zone.
Filled squares: The amphibolites of the Western Zone.
Filled circles: Schistose gabbro and brown hornblende amphibolite of the Axial Zone.
Open circles: Gneissose gabbro of the Axial Zone.
Triangles: Normal gabbro of the Eastern Zone.

(c) Various kinds of late phase biotite-hornblende rich leucocratic products, occuring as veins, schlierens or conformable bands, occur in the Type II gneissose gabbros but are virtually excluded from the Type I gneissose gabbro.

These features suggest that initial intrusive phase of the Type II gneissose gabbro was the fine-grained rock which was followed by that of the less basic coarse-grained gabbro which contained more volatiles as indicated by the presence of the leucocratic veins and bands.

The normal gabbro which includes olivine gabbro, pyroxene gabbro, hornblende gabbro and diorite, is characterized by a wide variation in grain size, with finer grained facies being intruded and partly replaced by coarser grained ones. In general, the fine-grained rocks have ophitic to xenomorphic granular texture, but are characterized by definite grain size and textural domains as has been described above. Domains of granular mineral association, compared of an olivine-plagioclase assemblage, are earlier than the ophitic plagioclase-pyroxene and/or hornblende domains as suggested by their respective mineral associations. The contacts between the domains are always gradational which suggests simultaneous, but heterogeneous crystallization with the more volatile rich parts being represented by the ophitic domains.

It is considered that the formation of separate granular and ophitic domains on a small scale reflect a much large process by which the coarser grained hornblende gabbro and diorite were formed. However, in some areas coarse-grained diorite was formed by migmatitization of previously consolidated gabbro. Such a process is complex and is, at present, not clearly understood. It is hoped that future study will shed more light onto this problem.

The septa rocks have been variously metamorphosed. Within gneissose gabbro the septa rocks are considerably basified with the formation of hypersthene and cordierite and those within normal gabbro have been thermally metamorphosed to form biotite bearing assemblages. The arrangement of the septa in each normal gabbro body suggests that they were the original wall rocks of a series of chambers which were successively intruded by magma to form olivine gabbro, pyroxene and hornblende gabbro.

Chemical Composition of the Basic Rocks

Wet chemical analysis of the basic plutonic rocks of the Hidaka Metamorphic Belt are tabulated (Tab. II). Analysis of granites and migmatites are excluded. Fig. 46 show the variation of major oxides in terms of $100 \times MgO/MgO + FeO + Fe_2O_3 + Na_2O + K_2O$ (S.I.). Despite various degrees of

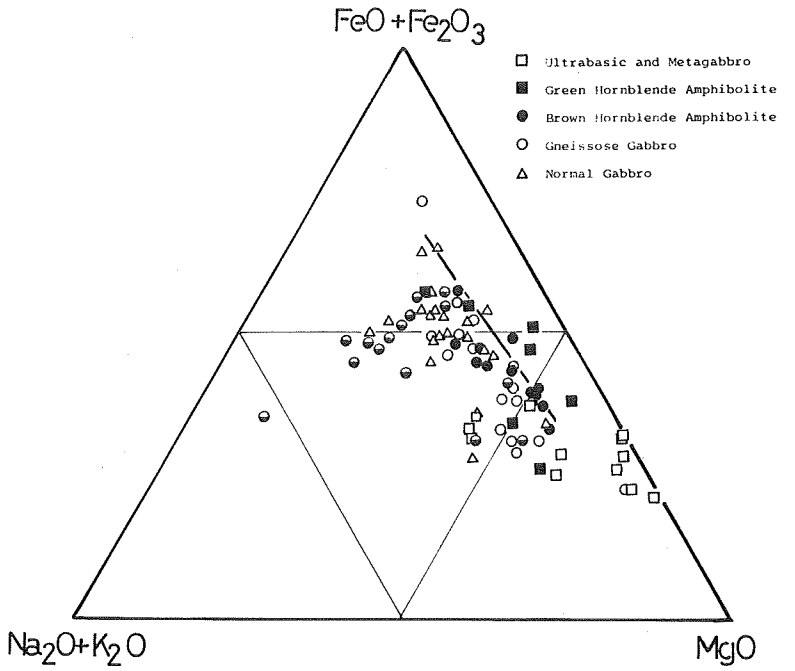

Fig. 46 A-F-M diagram of the Hidaka basic rocks.
The line indicates trend of the fine-grained rocks.
Open squares: Ultrabasic, layered gabbroic and metagabbro, rocks of the Western Zone.
Filled squares: Amphibolites of the Western Zone.
Filled circles: Schistose gabbro and brown hornblende amphibolite of the Axial Zone.
Open circles: Gneissose gabbro of the Axial Zone.
Triangles: Normal gabbro of the Eastern Zone.
Half filled circles: Septa rocks.

metamorphism the rocks show steady variational trends for each oxide.

With differentiation in the rocks of Stem I there is a marked increase in CaO, Al_2O_3 and Na_2O and a small increase in TiO_2. SiO_2 show a slight decrease to around S.I. 70 and then an increase. FeO + Fe_2O_3 show an increase to around S.I. 70 and then decrease. There is notable decrease in MgO. K_2O shows no variation. These variations mainly reflect a decrease in the amount of olivine and increase in the amount of plagioclase.

In the rocks of Stem II, CaO, MgO and Al_2O_3 show a slight decrease. FeO + Fe_2O_3, SiO_2 slightly increase and there is a notable increase in TiO_2, Na_2O and K_2O. These trends reflect as increasing proportion of plagioclase + hornblende with respect to olivine + pyroxene. Titania variation is mainly controlled by the amount of sphene + ilumenite. The somewhat large scatter of points in the Na_2O and K_2O diagrams may, in part, be the result of analytical

error in some of the earlier alkali determination by means of the Laurence-Smith method which is apt to produce erratic values.

Around S.I. 65 there is a compositional gap which marks a change in the slope of oxide variation, especially in the CaO, MgO, Al_2O_3 curves. This change in slope reflects the trasition from predominantly olivine + Plagioclase crystallization to predominantly plagioclase + pyroxene crystallization. The rock compositions are plotted on an AMF diagram (Fig. 47) and show that the olivine bearing Stem I rocks which plot near the M apex are separated into two groups as already stated above. Rock of Stem II cluster near the M-F boundary. The fine-grained gabbros show a distinct trend of Fe-enrichment.

Acknowledgements

The writer wish to express his sincere thanks to Prof. M. Hunahashi for his continuing help, advice and inspiration from the beginning of research on the Hidaka Metamorphic Belt. The writer is also much indebted to Prof. M. Minato for his continuing guidance and encouragement. He would like to acknowledge to Drs. S. Sako and M. Suzuki of the Geological Survey of Hokkaido, for their criticism and discussion. The writer is greatly helped by Dr. R.H. Grapes in the correction of english and his helpful discussion. Thanks are due to Miss K. Ishiyama and Messers H. Ohta dnd I. Watanabe who assisted him in the preparation of the manuscript.

Table II

	Peridotite									Layered Metagabbro	
	1	2	3	4	5	6	7	8	9	10	11
SiO_2	39.31	41.42	43.98	44.67	44.55	43.66	44.13	42.67	41.71	42.08	42.16
TiO_2	.00	.05	.15	.07	.10	.25	.12	.11	.10	.10	.30
Al_2O_3	1.27	1.12	3.75	4.75	4.21	1.05	2.56	4.91	1.31	14.58	6.62
Fe_2O_3	4.37	1.34	2.14	.48	.68	.83	1.90	.61	1.39	3.06	5.45
FeO	7.27	6.23	7.00	7.13	5.96	6.98	6.79	6.44	5.84	5.18	7.66
MnO	–	–	–	–	–	–	–	–	–	.14	.22
MgO	38.89	47.34	39.26	38.87	38.44	44.49	39.92	38.87	44.40	25.88	28.07
CaO	6.52	.79	2.45	2.84	3.28	1.72	3.79	2.78	.69	6.32	6.03
Na_2O	.04	.11	.03	.27	.27	.15	.32	.39	.09	.82	.31
K_2O	.14	.00	.00	.01	.01	.00	.00	.02	.00	.04	.01
P_2O_5	–	–	–	–	–	–	–	–	–	–	–
H_2O+	1.93	1.51	.79	.85	1.23	.62	1.10	3.06	3.96	1.86	1.99
H_2O-										.14	.31
Total	99.74	99.91	99.82	99.94	98.73	99.75	100.63	99.86	99.49	100.15	99.13
Anal.	S.H.	N.K.	N.K.	N.K.	N.K.	N.K.	N.K.	N.K.	N.K.	S.H.	S.H.
Q	.00	.00	.00	.00	.00	.00	.00	.00	.00	.00	.00
C	.00	.00	.00	.00	.00	.00	.00	.00	.00	.00	.00
Or	.78	.00	.00	.06	.06	.00	.00	.11	.00	.11	.00
Ab	.31	.89	2.52	2.25	2.25	1.26	2.67	3.25	.73	3.25	.73
An	2.89	2.56	8.87	11.71	10.24	2.17	5.56	11.60	3.17	11.60	3.17
Wo	12.29	.56	1.36	.99	2.51	2.65	5.52	.91	.10	.91	.10
En	.62	5.67	18.48	17.31	19.40	14.45	15.00	10.42	14.31	10.42.	14.31
Fs	.05	.49	2.04	2.24	2.07	1.52	1.61	1.19	1.21	1.19	1.21
Fo	68.30	78.62	55.55	55.69	53.47	67.49	59.15	60.52	67.44	60.52	67.44
Fa	7.65	7.54	6.78	7.97	6.28	7.86	7.01	7.67	6.30	7.67	6.30
Mt	6.32	1.92	3.10	.69	.97	1.18	2.73	.88	2.01	.88	2.01
Il	.00	.09	.27	.12	.18	.47	.23	.20	.18	.20	.18
Ap	.00	.00	.00	.00	.00	.00	.00	.00	.00	.00	.00

Table II continued

	Layered Metagabbro		Metagabbro			Gabbroic amphibolite					
	12	13	14	15	16	17	18	19	20	21	22
SiO_2	40.22	49.52	47.67	49.16	42.95	49.17	47.55	48.89	45.34	47.58	44.45
TiO_2	.19	.09	.21	.30	.17	.20	.18	.22	.17	.25	1.23
Al_2O_3	7.73	19.17	26.10	17.77	17.36	23.28	24.25	22.47	21.26	19.72	15.22
Fe_2O_3	4.90	2.38	1.38	1.12	2.36	.28	1.17	1.66	1.01	2.15	9.88
FeO	7.89	3.94	1.86	3.29	5.93	2.84	2.84	2.64	5.44	5.12	5.03
MnO	.19	.03	–	.11	.11	.08	.06	.06	–	–	–
MgO	32.18	8.82	4.60	9.26	22.14	7.67	5.33	5.33	11.87	9.37	12.90
CaO	2.16	13.19	14.35	14.56	7.59	14.97	14.12	14.54	13.17	13.00	9.43
Na_2O	.51	2.00	2.05	1.72	1.22	1.74	2.82	2.55	1.97	1.88	1.07
K_2O	.11	.02	.19	.03	.10	.00	.02	.04	.20	.38	.17
H_2O+	4.34	.98	1.00	1.65	.88	1.19	1.85	1.44	.87	.12	.77
H_2O-	.39	.13	.38	.15	.12	.94	.20	.16		.32	
Total	100.28	100.34	99.79	99.12	100.93	100.38	100.39	100.00	101.30	99.89	100.15
Anal.	S.H.	S.H.	S.H.	S.H.	S.H.	S.H.	S.H.	S.H.	S.H.	S.H.	S.H.
Q	.00	.00	.00	.00	.00	.00	.00	.00	.00	.00	.00
C	2.85	.00	.00	.00	1.46	.00	.00	.00	.00	.00	.00
Or	.61	.11	1.11	.17	.56	.00	.11	.22	1.17	2.23	1.00
Ab	4.30	16.88	17.30	14.52	10.28	14.68	23.80	21.55	16.62	15.89	9.02
An	10.71	43.28	61.45	40.67	37.64	55.72	53.46	49.74	48.59	44.26	36.22
Wo	.00	9.23	4.05	13.17	.00	7.73	6.91	9.34	6.98	8.44	4.40
En	17.74	18.79	7.59	19.32	2.27	6.26	1.18	8.23	6.24	8.43	31.72
Fs	2.35	4.42	1.27	4.04	.36	1.57	.36	2.01	1.87	2.60	1.25
Fo	43.72	2.22	2.70	2.61	37.04	8.98	10.13	3.52	25.09	10.43	.27
Fa	6.40	.57	.50	.59	6.56	2.49	3.41	.94	8.30	3.54	.01
Mt	7.09	3.45	1.99	1.62	3.40	.39	1.69	2.39	1.46	3.10	14.31
Il	.35	.17	.39	.56	.32	.38	.33	.41	.32	.47	.23
Ap	.00	.00	.00	.00	.00	.00	.00	.00	.00	.00	.00

Table II continued

	Green hornblende amphibolite				Brown hornblende amphibolite					Schistose gabbro	
	23	24	52	26	27	28	29	30	31	32	33
SiO_2	48.17	48.34	49.27	50.83	49.71	50.29	47.31	47.15	49.38	49.28	48.01
TiO_2	.74	.56	1.22	.150	1.44	.56	.52	1.34	1.03	.50	1.19
Al_2O_3	7.75	12.81	14.42	14.08	15.72	14.71	18.40	18.46	15.39	15.17	17.07
Fe_2O_3	2.84	4.76	4.22	3.33	4.57	1.49	2.23	.32	2.42	2.65	8.83
FeO	9.36	6.69	9.86	9.04	7.21	8.31	6.50	8.58	9.25	7.90	1.20
MnO	–	–	.13	–	–	.11	.10	–	–	.14	.19
MgO	14.76	10.92	6.18	7.46	6.13	9.06	7.62	11.19	8.67	8.67	12.60
CaO	12.49	13.06	8.34	9.38	9.89	10.95	11.87	10.07	8.80	11.42	8.62
Na_2O	1.01	1.42	4.44	2.63	1.13	3.17	3.08	1.94	2.47	3.25	2.14
K_2O	.38	.18	.06	.19	1.39	.24	.14	.53	1.68	.03	.09
P_2O_5	–	–	.07	–	–	.03	.05	–	–	.03	–
H_2O+	1.81	1.49	1.48	2.57	3.32	1.30	1.58	.23	1.07	1.36	.86
H_2O-	.04		.02		.32	.09	.04	.19	.16	.15	.10
Total	99.35	100.23	99.71	101.01	100.83	100.31	99.44	99.94	100.32	100.45	100.90
Anal.	S.H.	S.H.	S.H.	S.H.	S.H.	S.H.	S.H.	S.H.	S.H.	S.H.	S.H.
Q	.00	.00	.00	2.87	7.63	.00	.00	.00	.00	.00	2.37
C	.00	.00	.00	.00	.00	.00	.00	.00	.00	.00	.00
Or	2.23	1.06	.33	1.11	8.18	1.39	.78	3.12	9.91	.17	.50
Ab	8.49	12.01	37.54	22.23	9.54	26.79	26.01	16.41	20.87	27.47	18.09
An	15.52	28.04	19.25	26.04	33.71	25.20	35.99	40.08	25.95	26.70	36.72
Wo	19.38	15.33	9.09	8.55	6.40	12.08	9.44	4.11	7.39	12.43	2.52
En	26.24	26.39	5.52	18.57	15.26	9.38	1.66	7.49	9.34	7.55	31.37
Fs	9.72	7.20	4.62	11.38	7.08	5.53	.82	3.56	5.75	4.10	6.69
Fo	7.36	.56	6.90	.00	.00	9.22	12.13	14.26	8.57	9.83	.00
Fa	3.00	.16	6.35	.00	.00	5.99	6.63	7.49	5.82	5.89	.00
Mt	4.10	6.90	6.11	4.82	6.62	2.15	3.22	.46	3.50	3.82	12.78
Il	1.40	1.06	2.31	2.84	2.73	1.06	.99	2.53	1.94	.94	2.25
Ap	.00	.00	.13	.00	.00	.07	.10	.00	.00	.07	.00

Table II continued

	Schistose gabbro			Type I Gneissose Olivine gabbro						
	34	35	36	37	38	39	40	41	42	43
SiO_2	48.65	47.61	50.22	49.42	48.82	49.33	47.32	48.66	46.85	48.67
TiO_2	.81	1.62	.61	.58	.54	.48	.17	.24	2.15	.79
Al_2O_3	13.26	16.05	19.44	19.99	19.94	15.47	26.59	19.25	13.09	19.57
Fe_2O_3	1.67	3.13	2.16	1.88	.46	1.56	.48	.98	2.38	1.30
FeO	8.62	9.49	7.21	3.64	4.13	6.00	2.77	4.69	8.85	6.26
MnO	–	–	–	.09	.08	.13	.05	.09	–	–
MgO	14.89	7.35	8.18	8.15	7.71	10.50	5.96	10.11	14.20	9.00
CaO	8.89	11.52	10.46	11.58	13.31	12.62	13.66	12.53	8.81	12.03
Na_2O	1.97	2.39	1.32	2.84	2.50	2.18	1.93	2.23	3.58	2.04
K_2O	.96	.16	.34	.26	.18	.18	.04	.21	.29	.98
P_2O_5	–	–	–	.44	.40	.20	–	–	–	–
H_2O+	–	1.17	.36	.89	.84	.43	.72	1.02	.28	–
H_2O-	–	.22	.01	.71	.38	.32	.40	.44	.38	.10
Total	99.72	100.71	100.27	100.47	99.29	99.40	100.09	100.22	100.86	100.74
Anal.	Y.Y.	S.H.	Y.Y.	S.H.	S.H.	S.H.	S.H.	S.H.	S.H.	Y.Y.
Q	.00	.00	3.18	.00	.00	.00	.00	.00	.00	.00
C	.00	.00	.00	.00	.00	.00	.00	.00	.00	.00
Or	5.62	.88	2.00	1.50	1.06	1.06	.22	1.22	1.67	5.79
Ab	16.62	20.19	11.12	24.01	21.13	18.40	16.31	19.03	30.25	17.25
An	24.53	32.63	46.12	41.03	42.64	31.90	66.48	41.78	24.67	41.33
Wo	8.16	10.23	2.40	5.80	8.78	12.32	.52	8.50	7.93	7.65
En	12.36	12.27	20.37	11.97	9.15	15.65	4.13	8.40	9.22	6.30
Fs	4.37	8.17	10.45	2.56	3.07	5.49	1.25	2.52	3.72	2.56
Fo	17.31	4.22	.00	5.82	7.03	7.34	7.50	11.75	31.24	11.27
Fa	6.74	3.09	.00	1.36	2.61	2.84	2.50	3.88	13.89	5.05
Mt	2.41	4.52	3.13	2.71	.65	2.25	.69	1.41	3.45	1.88
Il	1.53	3.07	1.15	1.09	1.02	.91	.32	.46	.00	1.49
Ap	.00	.00	.00	1.01	.94	.47	.00	.00	.00	.00

Table II continued

	Type I Gneissose Olivine gabbro						Type I Gneissose gabbro and norite				
	44	45	46	47	48	49	50	51	52	53	54
SiO_2	48.57	48.87	47.43	49.46	51.53	50.41	50.88	51.36	48.53	53.24	51.18
TiO_2	.18	.15	.14	.14	.76	.36	1.18	1.16	.83	.70	.96
Al_2O_3	16.62	18.68	20.19	18.81	15.31	16.08	16.12	17.36	16.88	16.05	18.81
Fe_2O_3	.87	1.86	.85	.65	.71	1.18	2.43	.55	.64	1.99	1.36
FeO	6.81	4.50	6.45	6.13	8.01	8.33	8.57	7.50	8.26	6.65	8.69
MnO	–	–	–	–	–	–	.13	.18	.13	.11	–
MgO	11.56	9.20	11.33	8.96	7.12	7.05	8.76	10.38	10.42	9.67	6.86
CaO	12.13	12.83	10.63	13.05	12.24	13.61	8.70	9.10	10.68	8.44	9.34
Na_2O	2.22	2.56	2.28	2.35	2.92	2.53	3.18	1.90	2.59	2.65	2.93
K_2O	.07	.03	.08	.06	.19	.07	.36	.12	.15	.19	.43
P_2O_5	–	–	–	–	–	–	.16	.00	.12	.14	–
H_2O+	1.22	.76	1.34	.87	1.15	1.08	.97	.84	1.10	.98	.32
H_2O-							.21	.13	.19	–	
Total	100.22	99.44	100.22	100.48	99.94	100.70	101.65	100.58	100.52	100.81	100.88
Anal.	S.H.	S.H.	N.K.	N.K.	N.K.	N.K.	S.H.	S.H.	S.H.	S.H.	S.H.
Q	.00	.00	.00	.00	.00	.00	.00	1.04	.00	2.71	.00
C	.00	.00	.00	.00	.00	.00	.00	.00	.00	.00	.00
Or	.39	.17	.45	.33	1.11	.39	2.11	.67	.83	1.11	2.50
Ab	18.77	21.65	19.24	19.87	24.70	21.39	26.90	16.04	21.86	22.39	24.75
An	35.19	39.39	44.64	40.58	28.09	32.32	28.65	38.50	34.02	31.35	36.91
Wo	10.42	10.12	3.37	10.08	13.61	14.68	5.67	2.76	7.63	4.06	3.93
En	9.23	9.07	5.09	9.30	13.84	11.57	15.20	25.85	8.35	24.07	13.56
Fs	3.68	2.57	1.97	4.38	10.04	9.06	8.36	11.73	4.34	9.62	10.51
Fo	13.69	9.69	16.19	9.10	2.72	4.18	4.63	.00	12.32	.00	2.46
Fa	6.02	3.01	6.90	4.72	2.17	3.60	2.80	.00	7.07	.00	2.10
Mt	1.25	2.69	1.23	.93	1.02	1.69	3.52	.79	.93	2.87	1.97
Il	.33	.27	.26	.26	1.44	.68	2.23	2.20	1.56	1.32	1.82
Ap	.00	.00	.00	.00	.00	.00	.37	.00	.27	.30	.00

Table II continued

	Type I Gneissose gabbro and norite					Type II Gneissose gabbro		Olivine gabbro		Pyroxene gabbro	
	55	56	57	58	59	60	61	62	63	64	65
SiO_2	54.24	46.49	50.64	48.36	49.98	53.65	52.10	46.96	46.64	51.79	51.92
TiO_2	.91	2.12	1.89	2.00	.69	1.58	1.18	1.31	.49	3.40	1.36
Al_2O_3	17.61	17.92	20.60	21.07	14.42	16.90	15.14	11.50	23.54	16.29	17.64
Fe_2O_3	3.27	.60	2.68	2.74	3.81	.45	5.25	3.23	2.26	2.54	1.63
FeO	7.40	16.05	5.37	7.00	6.82	8.93	7.12	7.52	3.53	10.35	7.38
MnO	–	–	–	–	.13	–	–	–	–	–	–
MgO	5.05	3.81	6.02	6.45	10.13	5.90	7.01	17.26	6.92	4.50	6.52
CaO	5.87	9.04	9.28	8.96	9.71	8.37	9.34	7.81	11.63	6.98	9.79
Na_2O	3.25	2.24	3.21	2.18	2.27	3.01	2.84	2.55	2.29	1.92	2.13
K_2O	.71	.20	.31	.26	.24	.65	.61	.97	.90	.48	.68
P_2O_5	–	–	–	–	.12	–	–	–	–	–	–
H_2O+	.60	.62	.31	1.03	1.15	.46	–	1.44	1.47	.49	.82
H_2O-	.52	.17	.07		.45	.15	–			.84	.18
Total	99.43	99.26	100.38	100.05	99.90	100.05	100.59	100.58	99.71	99.58	100.05
Anal.	S.H.	S.H.	S.H.	S.H.	S.H.	S.H.	S.H.	S.H.	S.H.	Y.Y.	S.H.
Q	8.29	.00	1.05	2.63	.50	3.20	3.97	.00	.00	12.10	4.34
C	.84	.00	.00	.93	.00	.00	.00	.00	.00	.00	.00
Or	4.17	1.17	1.78	1.50	1.39	3.84	3.56	5.68	5.29	2.78	4.01
Ab	4.17	1.17	27.11	18.40	19.19	25.43	24.01	21.55	19.35	16.20	17.98
An	29.10	38.25	40.92	44.42	28.46	30.68	26.76	17.08	51.29	34.44	36.58
Wo	.00	2.74	2.13	.00	8.22	4.52	8.16	9.04	2.66	.07	4.99
En	12.57	6.74	14.99	16.06	25.22	14.68	17.45	4.38	1.05	11.10	16.23
Fs	9.39	18.14	4.54	7.29	8.24	13.42	6.79	.91	.22	11.29	9.96
Fo	.00	1.91	.00	.00	.00	.00	.00	27.04	11.33	.00	.00
Fa	.00	5.65	.00	.00	.00	.00	.00	6.22	2.76	.00	.00
Mt	4.72	.86	3.87	3.96	5.51	.65	7.60	4.68	3.26	3.68	2.36
Il	1.71	4.02	3.58	3.79	1.31	2.99	2.23	2.47	.93	6.45	2.58
Ap	.00	.00	.00	.00	.00	.00	.00	.00	.00	.00	.00

Tsble II continued

	Pyroxene gabbro							Hornblende gabbro			
	66*	67*	68	69	70	71	72	73*	74*	75*	76
SiO_2	53.34	52.49	51.19	50.73	51.90	51.30	52.23	53.80	51.57	51.36	57.16
TiO_2	1.07	1.09	2.38	1.13	1.64	.45	1.77	.64	1.35	.71	1.01
Al_2O_3	16.44	15.92	16.56	16.61	17.00	20.70	18.11	15.00	16.98	20.72	17.18
Fe_2O_3	2.93	3.22	3.01	4.44	5.02	.57	.73	4.95	2.03	1.49	3.63
FeO	7.14	7.53	8.16	7.16	7.34	3.29	8.16	7.41	8.14	6.48	4.75
MnO	–	–	–	–	–	–	–	–	–	–	–
MgO	6.43	7.06	5.14	7.71	4.07	6.48	5.58	6.42	6.44	6.66	4.01
CaO	9.02	9.13	9.22	9.65	10.26	13.17	9.65	10.97	9.15	10.58	7.04
Na_2O	3.12	1.55	2.84	2.60	2.32	2.58	3.14	3.51	3.30	1.61	2.45
K_2O	.55	.45	.53	.49	.42	.91	.43	.69	.38	.70	.76
P_2O_5	–	–	–	–	–	–	–	–	–	–	–
H_2O+	.50	.24	1.01	.10	.07	1.02	.55	.80	.86	.15	1.09
H_2O-	.42	.48		.01	.01	.24		.68		.49	
Total	100.96	99.16	100.04	100.63	100.05	100.98	100.35	99.87	100.20	100.95	99.13
Anal.	Y.Y.	S.H.	Y.Y.	Y.Y.	S.H.	Y.Y.	S.H.	S.H.	S.H.	Y.Y.	S.H.
Q	3.51	4.56	1.52	9.27	.00	9.63	1.15	.61	.00	3.58	17.42
C	.00	.00	.00	.00	.00	.00	.00	.00	.00	.00	.00
Or	3.23	3.12	2.89	2.45	5.34	2.62	2.50	4.06	2.23	4.12	4.45
Ab	16.20	17.98	26.37	24.01	21.97	19.61	21.81	13.11	26.53	29.68	27.89
An	29.23	30.88	32.21	34.74	42.22	35.16	34.07	23.14	30.40	47.26	33.63
Wo	6.47	6.20	6.53	6.74	9.64	4.23	5.75	13.05	6.25	2.17	.53
En	16.01	12.80	19.19	10.13	10.08	17.57	13.89	15.98	15.97	16.58	9.98
Fs	8.93	8.57	7.61	6.62	3.01	9.38	11.46	8.47	11.00	9.50	4.06
Fo	.00	.00	.00	.00	4.24	.00	.00	.00	.04	.00	.00
Fa	.00	.00	.00	.00	1.40	.00	.00	.00	.02	.00	.00
Mt	4.24	4.35	6.44	7.27	.81	4.65	1.04	7.16	2.94	2.15	5.26
Il	2.02	4.51	2.14	3.11	.85	2.06	3.35	1.21	2.55	1.34	1.91
Ap	.00	.00	.00	.00	.00	.00	.00	.00	.00	.00	.00

* Fine-grained Facies

Table II continued

	Hornblende gabbro				Diorite		Diabase porphyrite	Type I Septa			
	77	78	79	80	81	82	83	84	85	86	87
SiO_2	54.92	52.08	50.50	56.20	58.27	58.54	50.03	64.38	60.02	55.82	56.94
TiO_2	1.70	.73	1.26	1.01	1.15	.74	.99	.72	1.09	.42	.32
Al_2O_3	18.82	13.57	15.12	16.14	15.28	16.70	15.57	14.57	18.86	14.95	18.72
Fe_2O_3	3.19	5.46	3.52	2.90	4.19	2.15	1.23	1.23	1.22	2.60	1.92
FeO	4.97	6.69	7.19	6.56	5.62	6.23	7.73	5.50	7.13	7.97	5.46
MnO	–	–	–	–	–	–	–	.11	–	.14	.10
MgO	3.22	6.32	9.55	5.39	4.19	5.85	8.63	2.67	4.21	6.11	4.97
CaO	6.40	9.15	10.20	7.04	6.11	5.21	11.47	4.04	2.60	8.02	7.00
Na_2O	3.88	3.54	2.35	2.65	3.51	3.49	1.76	3.34	2.40	2.92	3.31
K_2O	1.07	.76	.56	.37	1.43	.71	.45	.91	.84	.22	.37
P_2O_5	–	–	–	–	–	–	–	.16	–	.18	.15
H_2O+	1.18	.93	.26	.46	.89	.84	1.63	1.53	.94	.89	.93
H_2O-		.53	.55	.73		.51	.15	.21	.18	.04	.09
Total	99.35	99.76	101.06	99.45	100.64	100.97	99.64	99.37	99.49	100.28	100.28
Anal.	S.H.	S.S.	S.H.	S.H.	S.H.	S.S.	S.H.	S.H.	S.H.	S.H.	S.H.
Q	8.32	2.34	.00	13.50	12.69	11.82	.56	25.62	26.35	9.22	10.58
C	.00	.00	.00	.00	.00	.71	.00	1.09	9.28	.00	.46
Or	6.29	4.45	3.28	2.17	8.40	4.17	2.62	5.34	4.95	1.28	2.17
Ab	32.82	29.94	19.87	22.39	29.68	29.52	14.84	28.21	20.29	24.70	28.00
An	30.76	18.89	29.04	31.04	21.72	25.84	33.30	19.11	12.88	27.04	33.88
Wo	.41	11.06	8.99	1.61	3.58	.00	9.85	.00	.00	4.90	.00
En	8.01	15.73	22.59	13.42	10.43	14.56	21.84	6.64	10.48	15.21	12.37
Fs	3.69	6.58	7.81	7.99	4.97	6.46	11.54	8.09	10.29	12.06	8.09
Fo	.00	.00	.82	.00	.00	.00	.00	.00	.00	.00	.00
Fa	.00	.00	.31	.00	.00	.00	.00	.00	.00	.00	.00
Mt	4.61	7.90	5.09	4.19	6.07	3.10	1.78	1.78	1.76	3.75	2.78
Il	3.22	1.38	2.38	1.91	2.17	1.40	1.87	1.37	2.06	.79	.61
Ap	.00	.00	.00	.00	.00	.00	.00	.37	.00	.40	.34

Table II continued

	Type II Septa	Type III Septa							
	88	89	90	91	92	93	94	95	96
SiO_2	62.45	62.25	57.29	53.60	66.08	61.30	64.35	73.14	60.51
TiO_2	.79	.90	.52	.49	.79	.88	.58	.26	.94
Al_2O_3	16.26	14.06	18.30	19.86	14.96	17.02	14.27	13.09	15.84
Fe_2O_3	2.84	2.34	2.49	2.34	2.13	1.80	2.56	1.31	4.57
FeO	5.22	6.74	7.01	9.07	4.77	5.71	4.48	1.43	4.85
MnO	–	–	.13	.14	.08	.14	.08	.02	.08
MgO	3.86	5.52	4.43	5.67	3.06	3.61	4.73	1.21	3.51
CaO	4.54	2.79	4.04	3.85	1.95	2.63	3.16	1.57	2.27
Na_2O	2.97	3.08	3.43	2.51	2.73	2.58	3.16	3.60	3.57
K_2O	.95	.85	1.54	.62	2.64	2.31	1.42	3.36	2.60
P_2O_5	–	–	.11	.07	–	–	.24	.10	.13
H_2O+	.75	–	.42	1.55	1.02	.94	.93	.84	1.05
H_2O-	.10	–	.15	–	.06	.22	.50	.02	.51
Total	100.73	98.53	99.86	99.86	100.27	99.14	100.46	99.95	100.43
Anal.	S.H.	S.H.	S.H.	S.H.	S.H.	S.H.	S.H.	S.H.	S.H.
Q	23.41	22.85	11.85	13.71	28.74	22.93	24.95	33.98	18.38
C	2.10	3.10	3.86	8.20	4.08	5.51	2.29	.91	3.31
Or	5.57	5.01	9.07	3.62	15.58	13.64	8.35	19.81	15.36
Ab	25.11	26.01	28.99	21.18	23.07	21.81	26.69	30.41	30.15
An	22.50	13.82	19.44	18.75	9.65	13.02	14.33	7.18	10.49
Wo	.00	.00	.00	.00	.00	.00	.00	.00	.00
En	9.61	13.74	11.02	14.11	7.62	8.98	11.77	3.01	8.73
Fs	5.95	8.97	10.20	14.17	5.84	7.80	5.30	1.15	3.73
Fo	.00	.00	.00	.00	.00	.00	.00	.00	.00
Fa	.00	.00	.00	.00	.00	.00	.00	.00	.00
Mt	4.10	3.38	3.59	3.38	3.08	2.59	3.70	1.90	6.62
Il	1.49	1.70	.99	.93	1.49	1.67	1.09	.49	1.78
Ap	.00	.00	.24	.13	.00	.00	.54	.24	.30

The Localities of Analized Samples

1. Mt. Tottabetsu 2. R. Wensaru 3. R. Wensaru 4. R. Wensaru 5. R. Wensaru 6. R. Pankenushi 7. R. Pankenushi 8. R. Wensaru 9. R. Wensaru 10. Mt. Poroshiri, Nukabira Cirque Wall 11. Mt. Poroshiri, Nukabira Cirque Wall 12. Nukabira Cirque Wall 13. Nakabira Cirque Wall 14. R. Pankenushi 15. Mt. Poroshiri Ridge 16. Mt. Poroshiri Ridge 17. Mt. Poroshiri Ridge 18. Mt. Poroshiri Ridge 19. Mt. Poroshiri Ridge 20. R. Pankenushi 21. R. Chiroro 22. Mt. Tottabetsu, Numa Cirque Wall 23. R. Niikappu 24. R. Chiroro 25. R. Niikappu 26. R. Pankenushi 27. R. Niobetsu 28. Mt. Esaomantottabetsu 29. Mt. Esaomatottabetsu 30. Mt. Esaomantottabetsu 31. R. Menashunbetsu 32. R. Chiroro 33. R. Niikappu 34. R. Tottabetsu 35. R. Niikappu 36. R. Tottabetsu 37. R. Pankenushi 38. R. Wensaru 39. R. Saru 40. R. Saru 41. R. Wensaru 42. R. Pankenushi 43. R. Tottabetsu 44. R. Pankenushi 45. R. Saru 46. R. Pankenushi 47. R. Pankenushi 48. R. Pankenushi 49. R. Pankenushi 50. E. Tottabetsu 51. R. Niikappu 52, R. Tottabetsu 53. R. Tottabetsu 54. R. Tottabetsu, Ju no sawa 55. R. Tottabetsu 56. R. Tottabetsu 57. R. Pankenushi 58. R. Pankenushi 59. R. Saru 60. R. Satsunai 61. Mt. Kamui 62. R. Tottabetsu, Showa-sawa 63, R. Oshirabetsu 64. R. Pirikapetan 65. R. Pirikapetan 66. R. Pirikapetan 67, R. Pirikapetan 68. R. Pirikapetan 69. R. Pirikapetan 70. R. Oshirabetsu 71. R. Tottabetsu 72. R. Tottabetsu 73, Oshirabetsu, average of 3 rocks 74. Showa-sawa 75. R. Pirikapetan 76. Oshirabetsu, average of 3 rocks 77. R. Tottabetsu 78. Mt. Tokachi-poroshiri 79. R. Tottabetsu 80. R. Tottabetsu 81. Taniiso, Oshirabetsu 82. R. Satsunai 83. R. Niobetsu 84. Mt. Tottabetsu 85. R. Niikappu 86. Mt. Tottabetsu 87. Mt. Tottabetsu 88. R. Tottabetsu, Hachi no sawa 89. R. Pirikapetan 90. R. Tottabetsu 91. R. Tottabetsu 92. R. Tottabetsu 93. R. Tottabetsu 94. R. Tottabetsu 95. R. Tottabetsu 96. R. Pirikapetan

Analist:
S.H.: S. Hashimoto H.S.: H. Sakurada N.K.: Nochi and Komatsu S.S.: S. Sako Y.Y.: Y. Yamashita

References

Hashimoto, S. (1949): On the Poroshiri-dake plutonic complex, northern Hidaka mountains, Hokkaido *Earth Sci.* 1.1-6.

Hashimoto, S. (1950): On the nickel bearing pyrrhotite and graphite deposits at Oshirabetsu, Tokachi Prov. Hokkaido. *Jour. Fac. Sci. Hokkaido Univ.* 7.227-236.

Hunahashi, M. (1948): Contact metasomatism associated with the pyroxene-peridotite of the Horoman region in Hidaka metamorphic zone, Hokkaido. *Jour. Fac. Sci. Hokkaido Univ.* 8.1-33.

Hunahashi, M. (1951): On the rocks of the Hidaka metamorphic zone and the Kamuikotan zone, Hokkaido. *Earth Sci.* 4.1-12.

Hunahashi, M. (1951): Cupriferous pyrrhotite deposit, "Saruru Mine". *Earth Sci.* 5.7-14.

Hunahashi, M., Hashimoto, S. (1951): Geology of the Hidaka zone. *Monogr. Geol. Collaboration.* 6.1-38.

Hunahashi, M. (1957): Alpine Orogenic Movement in Hokkaido, Japan. *Jour. Fac. Sci. Hokkaido Univ.* 9.415-467.

Igi, S. (1953): Petrographical studies on the peridotite in the Horoman region, southern end of the Hidaka mountain range, Hokkaido. *Jour. Geol. Soc. Japan.* 59.111-121.

Ishikawa, T. (1956): Jubilee publication commemor. Prof. J. Suzuki.

Jimbo, K. (1892): General geological sketch of Hokkaido. Hokkaido Pref. Office.

Kim, C. (1961): Facies variation of gabbro on the nickeliferous pyrrhotite deposits. *Jour. Jap. Assoc. Min. Petr. Econ. Geol.* 46.178-186.

Komatsu, M., Nochi, M. (1966): Ultrabasic rocks in the Hidaka Metamorphic Belt, Hokkaido. I.-Mode of occurrence of the Horoman ultrabasic rocks. *Earth Sci.* 87.21-29.

Minato, M., Yagi, K., Hunahashi, M. (1956): Geotectonic synthesis of the greentuff regions in Japan. *Bull. Earthq. Inst.* 34.237-264.

Minato, M., Gorai, M., Hunahashi, M. (1965): The geologic development of the Japanese island. Tsukiji Shoin. Tokyo.

Niida, K. (1974): Structure of the Horoman ultramafic massif of the Hidaka metamorphic Belt in Hokkaido, Japan. *Jour. Geol. Soc. Japan.* 80.31-44.

Nochi, M., Komatsu, M. (1967): Ultrabasic rocks in Hidaka Metamorphic Belt, Hokkaido II-Petrological relationships of the ultrabasic rocks and the olivine gabbro in the Wensaru-Pankenushi area. Earth Sci. 21.11-26.

Sako, S. (1963): On the relation between plutonism and ore mineralization in the Hidaka Metallogenetic Province, Hokkaido. Rep. Geol. Surv. Hokkaido. 30.1-49.

Suzuki, J. (1944): General view on the geology of Hokkaido. Jour. Geol.Soc. Japan. 51.15-24.

Suzuki, J. (1959): Petrological study of the Kamuikotan Metamorphic Complex in Hokkaido. Jour. Fac. Sci., Hokkaido Univ. 10.349-446.

Suzuki, M. (1963): On so-called schalstein in the Axial Zone of Hokkaido. Earth Sci. 63.15-22.

Watanabe, J. (1961): On the amphibolitic rocks of the upper course of the syumbetsu River, Hidaka, Hokkaido. Jour. Jap. Assoc. Min. Petro. Econ. Geol. 46.213-222.

(Manuscript recieved November 6, 1974)

The Western Zone

- Green schist
- Epidote amphibolite and Green hornblende schistose amphibolite
- Metagabbro including Layered gabbro and Gabbroic amphibolite
- Green hornblende amphibolite
- Peridotite

The Axial Zone

- Biotite schist and Schistose hornfels
- Biotite gneiss and Plagioclase porphyroblastic biotite gneiss
- Migmatite (Tonalitic rock)
- Granitic migmatite and Gneissose granite
- Brown hornblende amphibolite
- Biotite hornblende gneiss
- Gneissose olivine gabbro and Gneissose norite

The Eastern Zone

- Olivine gabbro, Gabbro and Diorite
- Aplite
- Septa
- Granite
- Layered gabbro

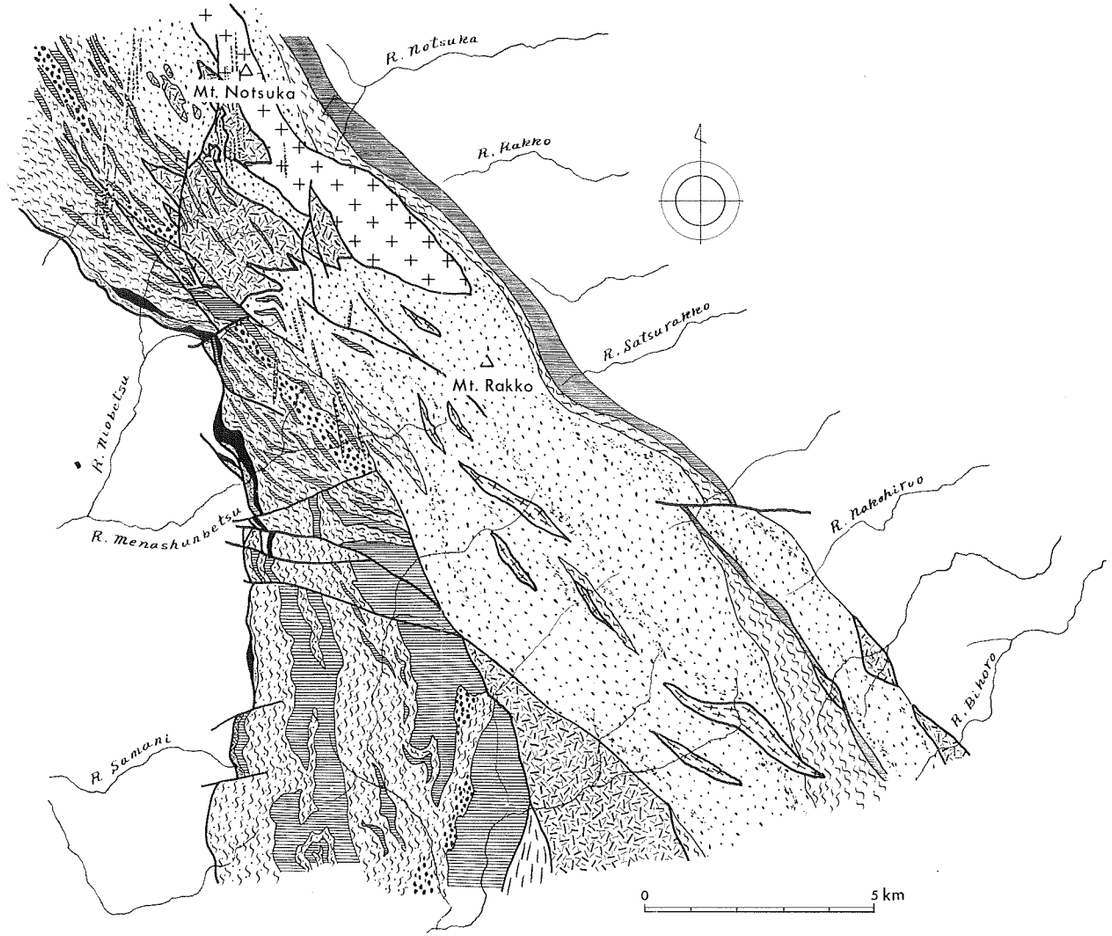

- Green schist and Epidote amphibolite
- Peridotite
- Biotite schist and Schistose hornfels
- Plagioclase porphyroblastic Biotite gneiss
- Banded Biotite gneiss
- Hypersthene bearing Migmatite
- Migmatite
- Granitic migmatite
- Brown hornblende amphibolite
- Gneissose norite
- Gabbro with Septa
- Granite
- Diabase porphyrite